

When is Multicalibration Post-Processing Necessary?

Dutch Hansen*
University of Southern California
jmhansen@usc.edu

Siddhartha Devic*
University of Southern California
devic@usc.edu

Preetum Nakkiran
Apple
preetum@nakkiran.org

Vatsal Sharan
University of Southern California
vsharan@usc.edu

Abstract

Calibration is a well-studied property of predictors which guarantees meaningful uncertainty estimates. Multicalibration is a related notion — originating in algorithmic fairness — which requires predictors to be simultaneously calibrated over a potentially complex and overlapping collection of protected subpopulations (such as groups defined by ethnicity, race, or income). We conduct the first comprehensive study evaluating the usefulness of multicalibration post-processing across a broad set of tabular, image, and language datasets for models spanning from simple decision trees to 90 million parameter fine-tuned LLMs. Our findings can be summarized as follows: (1) models which are calibrated out of the box tend to be relatively multicalibrated without any additional post-processing; (2) multicalibration post-processing can help inherently uncalibrated models; and (3) traditional calibration measures may sometimes provide multicalibration implicitly. More generally, we also distill many independent observations which may be useful for practical and effective applications of multicalibration post-processing in real-world contexts.

1 Introduction

A popular approach to ensuring that probabilistic predictions from machine learning algorithms are *meaningful* is model calibration. Intuitively, calibration requires that amongst all samples given score $p \in [0, 1]$ by an ML algorithm, exactly a p -fraction of those samples have positive label. Calibration ensures that a predictor has an accurate estimate of its own predictive uncertainty, and is a fundamental requirement in applications where probabilities may be taken into account for high-stake decisions such as disease diagnosis (Dahabreh et al., 2017) or credit/lending decisions (Bequé et al., 2017). Miscalibration can result in undesirable downstream consequences when probabilistic predictions are *thresholded* into decisions: if a predictor has high calibration error in disease diagnosis, for example, the individuals assigned lower predicted probabilities may be unfairly denied treatment. Calibration has a long history in the machine learning community (Guo et al., 2017; Minderer et al., 2021; Niculescu-Mizil and Caruana, 2005; Platt et al., 1999), but was arguably first introduced in *fairness* contexts by Cleary (1968). More recently, it has appeared in the algorithmic fairness community via the seminal works of Chouldechova (2017); Kleinberg et al. (2017).

Although calibration ensures meaningful uncertainty estimates aggregated over the entire population, it does *not* preclude potential discrimination at the level of *groups* of individuals: a model may be well calibrated overall but systematically underestimate the risk or qualification probability on historically underrepresented subsets of individuals. For example, Obermeyer et al. (2019) show differing calibration error rates across groups defined by race for prediction in high-risk patient care management systems. As pointed out by Obermeyer et al. (2019), in the

* Equal contribution.

downstream task of patient intervention based on thresholds over probabilistic predictions, this can inadvertently lead to differing rates of healthcare access based on group membership.

To combat these issues, the notion of *multicalibration* was proposed as a refinement of standard calibration (Hébert-Johnson et al., 2018). Multicalibration requires that a model be simultaneously calibrated on an entire collection of (efficiently) identifiable and potentially overlapping subgroups of the data distribution. A plethora of recent theoretical work has studied and utilized multicalibration to obtain interesting and important guarantees in algorithmic fairness (Bastani et al., 2022; Devic et al., 2024; Dwork et al., 2021; Gopalan et al., 2022b,c; Jung et al., 2021; Shabat et al., 2020), learning theory (Gollakota et al., 2024; Gopalan et al., 2023, 2022a), and cryptography (Dwork et al., 2023). Desirable consequences of multicalibrated predictors abound: multicalibration can provide provable guarantees on the transferability of a model’s predictions to different loss functions (omniprediction, Gopalan et al. (2022a)), the ability of a model to do meaningful conformal prediction (Jung et al., 2023), and universal adaptability or domain adaptation (Kim et al., 2022).

Although there is a host of theoretical results surrounding multicalibration and related notions, there is little systematic empirical study of the latent multicalibration error of popular machine learning models, the effectiveness of multicalibration post-processing algorithms, or even best practices for practitioners who wish to apply ideas and algorithms from the multicalibration literature. In particular, theoretical results are often concerned with multicalibration towards subgroups defined by potentially *infinite* hypothesis classes (Haghtalab et al., 2023; Hébert-Johnson et al., 2018), whereas fairness practitioners may only consider performance over a *finite* number of protected subgroups of interest, typically defined by attributes and meta-data normatively deemed as important (race, sex, ethnicity, etc. Chen et al. (2023)). Furthermore, most existing works applying multicalibration in practical settings only focus on one-off datasets or examples, and do not validate the algorithm across a variety of datasets and models or with realistic finite sample restrictions (Barda et al., 2020; La Cava et al., 2023; Liu et al., 2019).

To address these, we consider a “realistic” setup where a practitioner only has a finite amount of data, and must choose how to partition this data between learning and post-processing in order to achieve a suitable accuracy and multicalibration error rate over a finite set of subgroups. This allows us to investigate many important questions pertaining to the practical usage of multicalibration concepts and algorithms, which, to the best of our knowledge, have not been systematically previously considered by the theoretical or practical communities. For example, we can investigate the effectiveness of multicalibration post-processing algorithms and hyperparameter choices, as well as the latent multicalibration properties of popular machine learning models at a large scale.

More broadly, we initiate a systematic empirical study of multicalibration with the goal of answering the following two salient questions:

Question 1. In practice, how often and for what machine learning models is multicalibration an expected consequence of empirical risk minimization?

Question 2. Conversely, when must additional steps be taken to multicalibrate models, how difficult is this to do in practice, and what steps can be taken to make this easier?

The conventional wisdom is that multicalibration is something that is not naturally achieved by ML algorithms—this is precisely why many in the community have focused on creating post-processing algorithms which do achieve it (see e.g. Gopalan et al. (2022b); Hébert-Johnson et al. (2018), and Section 1.2). However, recent theoretical results suggest that multicalibration may in fact be an *inevitable consequence* of certain empirical risk minimization (ERM) methods with proper losses (Błasiok et al., 2023; Liu et al., 2019). This apparent conflict between conventional wisdom and recent results has not been tested in practice. We propose studying Question 1 since we believe that the current state of multicalibration in ML models should be systematically studied to better understand the implications for modern learning setups involving large models and fine-tuning. Question 2 is complementary and focused on investigating the effectiveness of current multicalibration algorithms on real datasets and illuminating challenges which can guide the development of future algorithms. A partial answer to one or both of these questions could help practitioners concerned about fairness understand when they should or should not expect multicalibration algorithms to improve fairness.

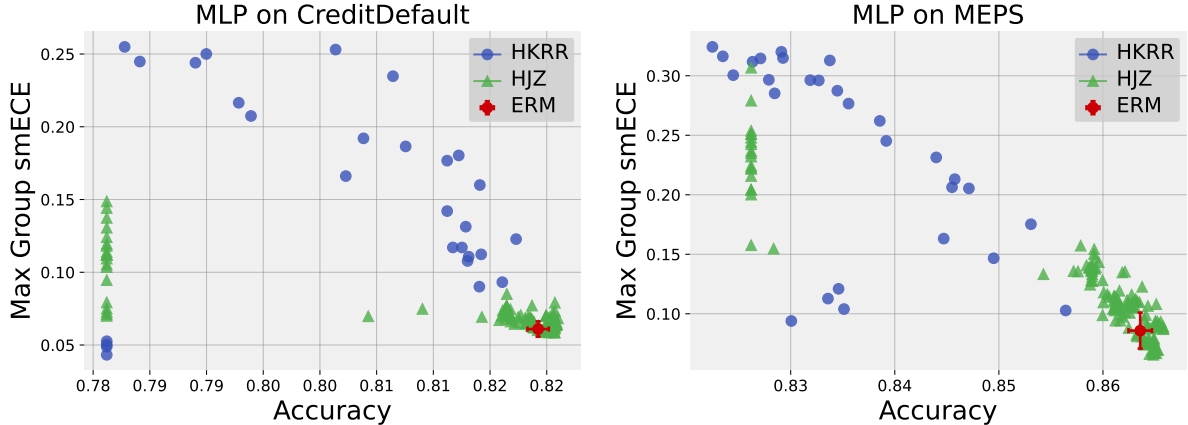


Figure 1: Test accuracy vs. maximum group-wise calibration error (smECE) averaged over five train/validation splits for MLP trained on CreditDefault and MEPS. Each point corresponds to the performance of the multicalibration post-processing algorithm HKRR (Hébert-Johnson et al., 2018) or HJZ (Haghtalab et al., 2023) with a different choice of hyperparameters. Standard empirical risk minimization (ERM) for MLPs achieves nearly optimal accuracy and multicalibration error.

1.1 Our Contributions

We conduct a large-scale evaluation of multicalibration methods, comparing three families of methods: (1) standard ERM, (2) ERM followed by a classical recalibration method (e.g. Platt scaling), and (3) ERM followed by an explicit multicalibration algorithm (e.g. that of Hébert-Johnson et al. (2018)).

We find that in practice, this comparison is surprisingly subtle: multicalibration algorithms do not always improve multicalibration (relative to the ERM baseline), for example. From the results of our extensive experiments on tabular, vision, and language tasks (involving running multicalibration algorithms more than 45K times), we extract a number of observations clarifying the utility of multicalibration. Most significantly, we find:

1. ERM alone is often a strong baseline, and can often be remarkably multicalibrated without further post-processing. In particular, on tabular datasets, multicalibration post-processing does not improve upon worst group calibration error of ERM for simple NNs.
2. Multicalibration algorithms are very sensitive to hyperparameter choices, and can require large parameter sweeps to avoid overfitting. These algorithms tend to be most effective in regimes with large amounts of available data, such as image and language datasets.
3. Traditional calibration methods such as Platt scaling or isotonic regression can sometimes give nearly the same performance as multicalibration algorithms, and are hyperparameter-free. Furthermore, compared to multicalibration post-processing, they are extremely computationally efficient and do not take very long to evaluate.

We also present numerous practical takeaways for users of multicalibration algorithms, which are not apparent from the existing theoretical literature, but are crucial considerations in practice. We believe that our investigations will not only broaden the practical applicability of multicalibration as a concept and algorithm, but also provide valuable information to the theoretical community as to what barriers multicalibration faces in practice. To both of these ends, all code used in our experiments is publicly accessible¹.

Organization. In Section 1.2, we begin with a brief review of related theoretical and experimental work in the multicalibration literature. We then detail our key experimental design choices in Section 2, before discussing our results on tabular data in Section 3. We extend our results to more complex image and language datasets in Section 4.

¹<https://github.com/dutchhansen/multicalibration>

Finally, we conclude with limitations of our experiments as well as practical takeaways for practitioners of fair machine learning in Section 5.

1.2 Related Works: Theory and Practice

The theory of multicalibration is rife with theoretical results investigating the sample complexity (Shabat et al., 2020), learnability, and computational efficiency of multicalibrated predictors. Hébert-Johnson et al. (2018) initiated this study by showing that achieving multicalibration over a hypothesis class \mathcal{C} defining protected subgroups requires access to a *weak agnostic learner* for that class (Shalev-Shwartz and Ben-David, 2014). From a fairness perspective, however, we are oftentimes—but not always (Sahlgren and Laitinen, 2020)—interested in subgroups defined by features or metadata, rather than a generic (and potentially infinite) hypothesis class. Subgroups in practical applications of algorithmic fairness are often given as input to the machine learning algorithm and intrinsic to a particular dataset of interest.

There is reason to believe that empirical risk minimization (ERM) on neural networks and other machine learning models may result in multicalibrated predictors. In recent works, Blasiok et al. (2024, 2023) prove that loss minimization with neural networks may yield multicalibrated predictors. Their proofs, however, may not be directly applicable to practice as they rely on an idealized optimization procedure. Nonetheless, both works echo a relationship between ERM and multicalibration also articulated in Liu et al. (2019), who show that group-wise calibration may be an inevitable consequence of well-performing models.

Although these results describe and prove links between ERM and multicalibration in theory, we systematically evaluate when this link holds in practice across a broad range of models. To the best of our knowledge, only Barda et al. (2021); La Cava et al. (2022) consider issues when applying multicalibration in practice. Both works are limited to small models or only run experiments with one or two datasets. Pfohl et al. (2022) measure subgroup calibration, but do not discuss it at length. Although the focus in Haghtalab et al. (2023) is mainly theoretical, the authors also run experiments for both their proposed multicalibration algorithms and additional algorithms present in the literature. However, they do not compare the performance of such algorithms against a baseline NN or tree-based method trained on an identical amount of data, and also do not investigate how much data should be used for training the base model vs. used for multicalibration post-processing. We believe such a comparison is important given that ERM may have latent multicalibration properties, and is by far the most used learning algorithm in practice.

In recent work, Detommaso et al. (2024) utilize multicalibration as a tool to improve the overall uncertainty and confidence calibration of language model but, to our knowledge, do not focus on or report fairness towards protected subgroups. Like us, they point out various issues with the standard multicalibration algorithm, which they address with early stopping and adaptive binning. We instead perform a large hyperparameter sweep which effectively implements an early stopping mechanism. We discuss this further in Appendix A.1. Nonetheless, our results for large models are complementary to those of Detommaso et al. (2024): both works demonstrate that (1) standard multicalibration can at times be difficult to get working in practice; and (2) ideas from the theoretical multicalibration literature can have impact at the scale of large models. We provide additional discussion of related works in model calibration and subgroup robustness in Appendix A.

2 Preliminaries

We work in the binary classification setting with a domain \mathcal{X} and binary label set $\mathcal{Y} = \{0, 1\}$, and assume data is drawn from a distribution \mathcal{D} over $\mathcal{X} \times \mathcal{Y}$. We consider arbitrary risk predictors $f : \mathcal{X} \rightarrow \Delta(\mathcal{Y})$, which return probability distributions over the binary label space. We will measure the calibration of f on a dataset $(X, Y) \in (\mathcal{X} \times \mathcal{Y})^n$ with the binned variant of the well-known and standard *Expected Calibration Error*, which we refer to as ECE (Guo et al., 2017). Throughout, we measure ECE with 10 bins of equal width 0.1.

Recent work has questioned ECE as a calibration measure, due to consistency and continuity issues that come with relying on a fixed bin width (Blasiok et al., 2023). To address these, we also report calibration as measured by *smoothed* ECE (smECE) (Blasiok and Nakkiran, 2023), which (1) can be roughly thought of as the ECE after applying a suitable

kernel-smoothing to the predictions, and; (2) satisfies desirable continuity and consistency guarantees (Błasiok et al., 2023; Błasiok and Nakkiran, 2023). Importantly, unlike binned ECE, there are no hyperparameters associated with measuring the smoothed calibration error. A full description of smECE is beyond the scope of our work—we refer the interested reader to Błasiok and Nakkiran (2023).

Multicalibration requires that a predictor have not only small calibration error overall, but also when restricted to marginal subgroup distributions of the data. In particular, we assume that there is a (finite) collection of groups $G = \{g_1, g_2, \dots\}$, where $g_i \subseteq \mathcal{X}$. We operationalize *measuring* multicalibration by reporting the *maximum* calibration error over a given collection of subgroups G . Taking the max avoids fairness concerns associated with the (weighted) mean of groups of varying size and/or degree of overlap. Note that the subgroup collection G is context and dataset dependent, and that the groups within G may be overlapping, capturing desirable *intersectionality* notions (Ovalle et al., 2023).

2.1 Multicalibration Post-Processing Algorithms and Hyperparameter Selection

In theory, standard calibration post-processing methods like Platt scaling (Platt et al., 1999) or temperature scaling (Guo et al., 2017) do not guarantee that predictions will be well-calibrated on protected subgroups. Therefore, in order to achieve multicalibration, Hébert-Johnson et al. (2018) propose an iterative boosting-style post-processing algorithm which we refer to as HKRR. The algorithm works by iteratively searching for and removing subgroup calibration violations until convergence. We detail the algorithm’s hyperparameters and the values we choose for them in Appendix D.1, and note that we perform a relatively wide parameter sweep.

The recent work of Haghtalab et al. (2023) also provide a *family* of alternative multicalibration algorithms with better theoretical sample complexity guarantees. This is motivated by the fact that HKRR is known to be theoretically *sample inefficient* (Gopalan et al., 2022b), and easily overfits (Detommaso et al., 2024). At a high level, each algorithm of Haghtalab et al. (2023) corresponds to a certain two-player game. Different algorithms in the family are a consequence of each player playing a different online learning algorithm. We detail the hyperparameters we over which we search in Appendix D.2, but note here that we use the same code and predominantly the same parameters reported by the authors. We refer to any (post-processing) algorithm in this family as HJZ.

In addition to these algorithms, we test the usefulness of three standard calibration techniques in reducing multicalibration error: Platt scaling (Platt et al., 1999), isotonic regression (Zadrozny and Elkan, 2002), and temperature scaling (Guo et al., 2017). The first two techniques are hyperparameter-free, and we use implementations given by Scikit-learn. We also use a parameter-free version of temperature scaling which we detail in Appendix D.3.

2.2 Experimental Methodology

Our investigation is primarily motivated by fairness desiderata. Therefore, we examine datasets where features or metadata allow us to naturally define meaningful collections of protected groups G . This includes five tabular datasets (ACS Income, UCI Bank Marketing, UCI Credit Default, HMDA, MEPS), two language datasets (Civil Comments, Amazon Polarity), and two image datasets (CelebA, Camelyon17). We detail and provide citations for each of our datasets and subgroups in Appendix C. For each dataset, we define between 10 and 20 overlapping subgroups depending on available features or metadata. For the tabular datasets, these subgroups are defined by features and conjunctions of features. For the image datasets, we use relevant metadata *not* available to the model in order to define subgroups. For the language datasets, we use the presence of meaningful words.

Data Partitioning. For consistency, we partition all datasets into three subsets: training, validation, and test. Test sets remain fixed across all experiments. We report accuracy and multicalibration metrics on the test set averaged over five splits of train and validation sets for tabular data, and three splits for more complex data. In each experiment where a multicalibration post-processing algorithm is used, we draw a holdout of variable size from our training set, which we term the *calibration set*. We term the fraction of our training set used in post-processing the *calibration fraction*. The calibration fractions over which we search appear in Appendix E.1 for tabular datasets and Appendix E.2 for image and language datasets.

The calibration set is used solely in multicalibration post-processing, and is *not* used in training a model prior to the post-process. This procedure is motivated by a need to measure the importance of *fresh* samples in multicalibration post-processing. If a model is already multicalibrated on its entire training set S , we *cannot* re-use S in HKRR or HJZ to improve the model, since the algorithms cannot improve on a predictor which is already perfectly multicalibrated on a particular dataset. This applies to models such as, for example, neural networks, which usually fit their training set to very low calibration error and high accuracy (Carrell et al., 2022). For these models, we also anticipate that the *multicalibration* error on the training set will be low, and hence, the data from S unusable for post-processing. Therefore, the calibration fraction itself is an important hyperparameter we consider. Ideally, in order to maximize the resulting accuracy of the final model, we would utilize as much data as possible for model training, and minimize the amount of data required for multicalibration post-processing. However, due to the sample complexity of multicalibration algorithms, we will see that finding this specific point can be difficult (see Figure 3).

Compute. All experiments were performed on a collection four AWS G5 instances, each equipped with a NVIDIA 24GB A10 GPU. We used only the CPU for multicalibration and calibration post-processing, which was by far the most computationally intensive task. We estimate that all of our experiments cumulatively took 10 days of running time on these four instances.

3 Experiments on Tabular Datasets

We begin our investigation with tabular data. All our results are computed with a mean and standard deviation over 5 train / validation splits. Although simpler than vision or language data, tabular data is an important and realistic setting which many algorithmic fairness practitioners encounter throughout the health, criminal justice, finance, and other sectors (Barda et al., 2021; Barenstein, 2019; Obermeyer et al., 2019). As our base predictors in this setting, we consider multilayer perceptron NNs (MLPs), DecisionTree and RandomForest, SVMs, NaiveBayes, and Logistic Regression. We defer dataset, group, and model details to Appendix C and Appendix E.1, but note that our datasets span from 10K examples (MEPS) to 200K (ACSIIncome). We instill the following insights from running multicalibration post-processing algorithms over 40,000 times on more than 1,000 separately trained models.

Observation 1: On tabular data, ML models which tend to be calibrated out of the box also tend to be multicalibrated without additional effort.

In Figure 1, we show the performance of every choice of multicalibration algorithm (corresponding to each choice of aforementioned hyperparameters) for MLPs on two datasets. We find that ERM performs nearly as well as the best set of hyperparameters across our wide parameter sweep. This is seen broadly across all of our tabular datasets for models which one may expect to be calibrated in practice, such as logistic regression or random forests². We include the complete plots of all multicalibration runs versus ERM in Appendix F.1.

We numerically verify Observation 1 by inspection of Figure 2. This table corresponds to the best choice of hyperparameters (according to maximum group-wise smECE on a validation dataset) of each method tested on the CreditDefault dataset. We find that HKRR and HJZ show no improvements to max ECE or max smECE for MLPs, random forests, and logistic regression. Multicalibration gains are also marginal (0 to 0.01) on the Bank Marketing, ACSIIncome, and Credit Default datasets (see Appendix F.2). On HMDA, however, multicalibration does seem to provide a noticeable improvement on the order of 0.03-0.05 for these models (Figure 21). We believe this is because ERM achieves worse *calibration* error on HMDA, possibly due to the increased difficulty of the dataset.

Observation 2: HKRR or HJZ post-processing can help un-calibrated models like SVMs or Naive Bayes achieve low group-wise maximum calibration error. Oftentimes, however, similar results can be achieved with traditional calibration methods like isotonic regression (Zadrozny and Elkan, 2002).

Across our datasets, we find that SVMs, Decision Trees, and Naive Bayes almost always have their max smECE error improve by 0.05 or more using post-processing. We also point out the relatively strong performance of isotonic regression and other traditional calibration methods across datasets and models. For example, isotonic regression

²We use a RF which predicts a *probability* corresponding to the fraction of positive points at the leaf.

provides nearly all the improvements (up to 0.01 error) of the multicalibration algorithms when applied to Naive Bayes in Figure 2. On the Credit default dataset in Figure 22, isotonic regression is — when considering standard deviation — tied with the *optimal* multicalibration post-processing algorithms for SVM and Naive Bayes. We have similar findings for the MEPS dataset and Random Forests trained on the HMDA dataset. Platt scaling and isotonic regression are desirable because they are *parameter-free* methods working out of the box without tuning, are simple for practitioners to implement, and further do not require large parameter sweeps to find effective models.

Model	ECE ↓	Max ECE ↓	smECE ↓	Max smECE ↓	Acc ↑
MLP ERM	0.022 ± 0.006	0.106 ± 0.009	0.024 ± 0.002	0.086 ± 0.015	0.864 ± 0.001
MLP HKRR	0.019 ± 0.005	0.122 ± 0.008	0.019 ± 0.004	0.104 ± 0.002	0.835 ± 0.003
MLP HJZ	0.019 ± 0.003	0.088 ± 0.011	0.021 ± 0.002	0.076 ± 0.018	0.864 ± 0.003
MLP Isotonic	0.02 ± 0.006	0.108 ± 0.021	0.02 ± 0.004	0.089 ± 0.021	0.864 ± 0.003
RandomForest ERM	0.019 ± 0.001	0.094 ± 0.006	0.021 ± 0.001	0.083 ± 0.004	0.863 ± 0.003
RandomForest HKRR	0.019 ± 0.005	0.122 ± 0.008	0.019 ± 0.004	0.104 ± 0.002	0.835 ± 0.003
RandomForest HJZ	0.021 ± 0.004	0.106 ± 0.011	0.021 ± 0.003	0.101 ± 0.012	0.86 ± 0.003
RandomForest Isotonic	0.015 ± 0.002	0.089 ± 0.014	0.017 ± 0.001	0.084 ± 0.014	0.862 ± 0.002
SVM ERM	0.143 ± 0.002	0.376 ± 0.012	0.072 ± 0.001	0.186 ± 0.006	0.857 ± 0.002
SVM HKRR	0.019 ± 0.005	0.122 ± 0.008	0.019 ± 0.004	0.104 ± 0.002	0.835 ± 0.003
SVM HJZ	0.031 ± 0.003	0.156 ± 0.021	0.027 ± 0.004	0.155 ± 0.02	0.828 ± 0.002
SVM Isotonic	0.048 ± 0.023	0.231 ± 0.085	0.048 ± 0.023	0.218 ± 0.069	0.847 ± 0.017
LogisticRegression ERM	0.022 ± 0.002	0.106 ± 0.008	0.022 ± 0.001	0.083 ± 0.003	0.866 ± 0.002
LogisticRegression HKRR	0.019 ± 0.005	0.122 ± 0.008	0.019 ± 0.004	0.104 ± 0.002	0.835 ± 0.003
LogisticRegression HJZ	0.021 ± 0.003	0.114 ± 0.019	0.023 ± 0.001	0.09 ± 0.011	0.866 ± 0.003
LogisticRegression Isotonic	0.017 ± 0.003	0.109 ± 0.019	0.019 ± 0.003	0.097 ± 0.02	0.863 ± 0.002
DecisionTree ERM	0.067 ± 0.004	0.261 ± 0.028	0.047 ± 0.004	0.166 ± 0.012	0.85 ± 0.006
DecisionTree HKRR	0.019 ± 0.005	0.122 ± 0.008	0.019 ± 0.004	0.104 ± 0.002	0.835 ± 0.003
DecisionTree HJZ	0.031 ± 0.003	0.156 ± 0.021	0.027 ± 0.004	0.155 ± 0.02	0.828 ± 0.002
DecisionTree Isotonic	0.014 ± 0.003	0.196 ± 0.026	0.015 ± 0.003	0.186 ± 0.027	0.838 ± 0.01
NaiveBayes ERM	0.277 ± 0.019	0.544 ± 0.02	0.164 ± 0.013	0.287 ± 0.011	0.714 ± 0.018
NaiveBayes HKRR	0.019 ± 0.005	0.122 ± 0.008	0.019 ± 0.004	0.104 ± 0.002	0.835 ± 0.003
NaiveBayes HJZ	0.031 ± 0.003	0.156 ± 0.021	0.027 ± 0.004	0.155 ± 0.02	0.828 ± 0.002
NaiveBayes Isotonic	0.019 ± 0.005	0.128 ± 0.017	0.021 ± 0.005	0.122 ± 0.015	0.831 ± 0.006

Figure 2: Best performing HKRR and HJZ post-processing algorithm hyperparameters (selected based on validation max smECE) compared to ERM on the MEPS dataset. Calibrated models (MLP, RandomForest, LogisticRegression) need not be post-processed to achieve multicalibration. However, uncalibrated models (SVM, Decision Trees, NaiveBayes) *do* benefit from multicalibration post-processing algorithms.

Observation 3: A practitioner utilizing multicalibration post-processing may have to trade off worst group calibration error and overall accuracy.

Due to the necessity of using hold-out data for running multicalibration post-processing, practitioners may have to choose between accuracy and worst group calibration error. For example, in Figure 3 we show that running multicalibration post-processing for MLPs on the HMDA dataset has a different optimal calibration fraction when considering accuracy and worst group calibration error as separate objectives. In fact, in this example, improving multicalibration error comes at a *cost* to accuracy of about 2%. Although small, this does indicate that the decision to use multicalibration post-processing here should be context dependent. Additional examples of this tradeoff include Decision Trees or Logistic Regression on most datasets (Figures 25 and 27). Plots for each dataset and model are in Appendix F.3.

Observation 4: On small datasets, there can be variations between smECE and the standard binned ECE.

To illustrate an example, ERM for Decision Trees on MEPS yields a worst group calibration error of 0.261 if calibration

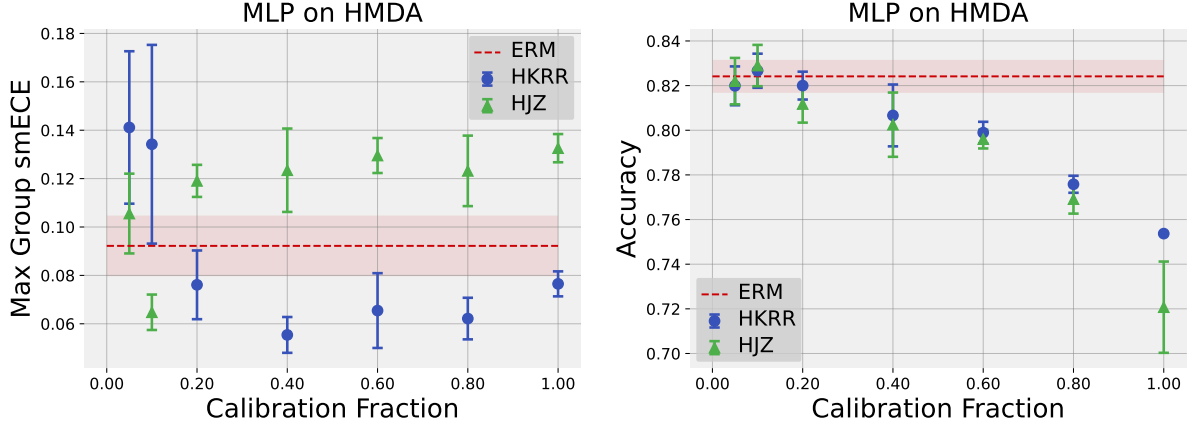


Figure 3: Hold-out calibration fraction vs. worst group calibration error (left) and accuracy (right) for MLPs on HMDA. Lowering worst group calibration error may come at a cost of model accuracy.

is measured using ECE, and 0.166 if using smECE (see Figure 2). This has important consequences for practitioners: if selecting the best model based on only the worst subgroup calibration error, the choice of *calibration metric* used will impact the choice of model. If selecting a post-processing algorithm based on ECE, HJZ may seem like a reasonable choice since it has a worst group ECE calibration error of 0.156. However, when using smECE to measure performance, HJZ does *not* significantly improve upon ERM.

We initially posited that this is because of the smaller sample sizes in some tabular datasets, but we note that even on the ACSIncome dataset with 200K examples, we find a significant difference of 0.1 between measuring the *overall* calibration error of SVMs with ECE vs. smECE (Figure 19). More generally, to avoid issues stemming from ECE bin choice, we recommend that practitioners utilize the smECE calibration measurement tool³ due to its theoretical guarantees and stability across our experiments.

Observation 5: There is no clearly dominant algorithm between HKRR and HJZ on tabular data, but HJZ is more robust towards the tested choice of hyperparameters.

Over the 30 experiments across all tabular datasets with all base models (Appendix F.2), HJZ and HKRR had statistically distinguishable performance on 24 runs. Amongst these 24, HJZ performed better 7 times. Nonetheless, we observe that the algorithm of HJZ is usually *less sensitive* to hyperparameter changes. In Figure 1 for example, the green points corresponding to hyperparameter choices for HJZ are tightly concentrated around ERM. We observe similar phenomena throughout additional model and dataset plots in Appendix F.1. Practitioners wishing to apply smaller hyperparameter searches over multicalibration algorithms may consider HJZ a suitable option, even if it gives slightly suboptimal worst group calibration error.

4 Experiments on Language and Vision Datasets

In this section, we evaluate the ability of multicalibration post-processing to improve upon the multicalibration of vision transformers, DistilBERT, ResNets, and DenseNets on a collection of image and language tasks. Our goal is to understand if multicalibration post-processing can help in more complicated, large model regimes within both the train-from-scratch and pre-trained paradigms.

As we move from smaller, tabular datasets to larger image and language datasets, we find that multicalibration algorithms may provide empirical improvements. Note here that in cases where we use a ResNet on language data, we train from scratch but use pretrained GloVe embeddings in the fashion of Duchene et al. (2023). In cases where we

³<https://github.com/apple/ml-calibration>

use a ResNet or DenseNet on image data, we also train from scratch. Whenever using a transformer, we finetune from pretrained weights (Dosovitskiy et al., 2021; Sanh et al., 2019). We defer further dataset, model, and group information to Appendix C and Appendix E.2.

Multicalibrating large models has an increased computational cost: For a single base predictor on tabular data, a full parameter sweep—training the multicalibration algorithm with every choice of hyperparameter—required 1-2 hours on a typical calibration set of 100K examples. With more complex base predictors (e.g. ResNets or language models) and larger datasets, this process takes significantly longer. Additionally, due to the increased computational cost of *re-training* a model in the image and language regimes, we only search over calibration fractions in $\{0.0, 0.2, 0.4\}$ and report our results averaged over three random train / validation splits. After running 1,700 multicalibration post-processing algorithms, we distill our findings into the following observations.

Observation 6: For image and language data, HKRR nearly always outperforms HJZ.

In all six of our experiments on image / language data (Appendix G.2), HKRR either matched or significantly beat the performance of HJZ. Note that we use the same parameter sweeps for HKRR and HJZ over image/language datasets that we used for the tabular datasets (see Appendix D), and leave open the possibility that HJZ may require a larger hyperparameter sweep to achieve good performance on more complex data.

Observation 7: Multicalibration post-processing can improve worst group smECE relative to an ERM baseline by 50% or more.

HKRR improved worst group calibration error in five out of six experiments. Among these five, the least improvement we saw was HKRR decreasing the worst group smECE of ERM from 0.06 to 0.043 (DistilBERT on Civil Comments). The greatest improvement we saw was from 0.07 to 0.02 (ViT on Camelyon17) and 0.09 to 0.05 (ResNet-56 on Amazon Polarity). These examples all appear in Figure 4. A full collection of tables and plots can be found in Appendix G.2.

Observation 8: Binned ECE and smECE provide nearly identical estimates of calibration error.

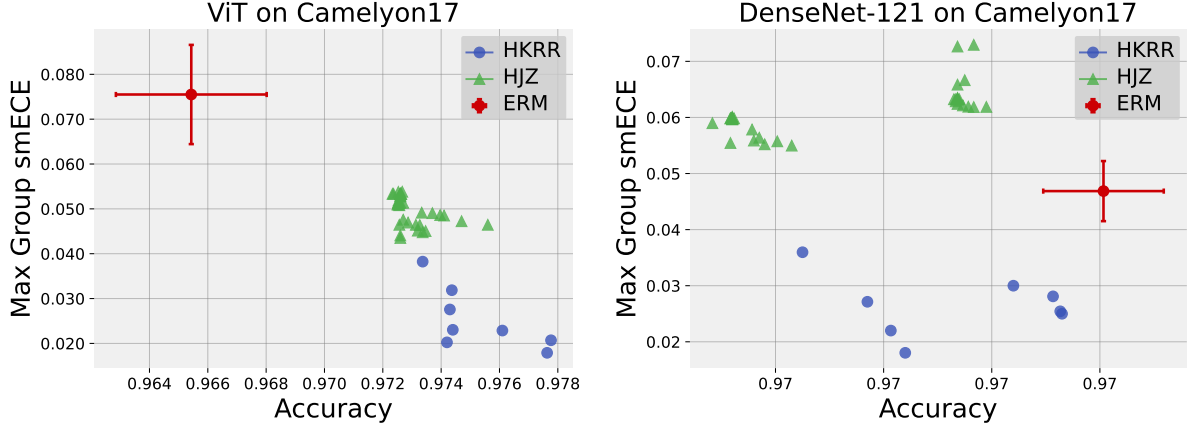
Among nearly all of our experiments on larger datasets of more than 100k examples, we were not able to find any datasets where the metric used to measure calibration error would change the outcome of chosen model (c.f. **Observation 4**).

5 Takeaways for Practitioners and Experimental Limitations

We now present some takeaways that span all of our experiments. First, we believe that the latent multicalibration of ERM has been generally underestimated for many models. In particular, on tabular datasets, multicalibration post-processing cannot improve upon ERM for MLPs (see **Observation 1**). Furthermore, the improvement offered for more complex image and language data is generally less than 0.05 smECE when considering standard deviation.

This directly motivates our next takeaway: Current multicalibration post-processing algorithms—when applied to calibrated models like neural networks—are extremely sensitive towards choice of hyperparameters, since the potential “scope” of improvement is on the scale of 0.02 to 0.03 smECE. The optimal hyperparameter choice for each algorithm largely varies by dataset and base model, and it takes quite a bit of granular searching to find the best performing algorithm, or indeed, an algorithm which improves upon ERM at all. For example, the optimal HJZ algorithm used at least 15 different hyperparameter configurations across only our 30 tabular experiments (when considering calibration fraction as an additional parameter); HKRR has similar sensitivity issues. Further, many hyperparameter choices do not seem to improve upon the ERM base model—for example, see DenseNet-121 in Figure 4 or the full multicalibration post-processing plots in Appendix G.1—making a significant portion of the hyperparameter sweeps not useful to perform. Since training HJZ or HKRR on a holdout of 100K examples can take 1-2 hours, it can be several hours before a suitable choice of hyperparameters is found. This computational cost is exacerbated in the larger regimes where multicalibration may be most useful, which poses a major obstacle for practical applications of either HKRR or HJZ.

As a direct stopgap measure, we recommend running and evaluating traditional calibration methods. As we point out in **Observation 2**, post-processing algorithms like isotonic regression can achieve nearly the performance of



Model	ECE ↓	Max ECE ↓	smECE ↓	Max smECE ↓	Acc ↑
DistilBERT ERM	0.021 ± 0.001	0.065 ± 0.005	0.021 ± 0.001	0.06 ± 0.004	0.915 ± 0.001
DistilBERT HKRR	0.013 ± 0.0	0.047 ± 0.005	0.013 ± 0.0	0.043 ± 0.004	0.915 ± 0.001
DistilBERT HJZ	0.004 ± 0.001	0.043 ± 0.008	0.007 ± 0.001	0.043 ± 0.007	0.915 ± 0.001
DistilBERT Isotonic	0.002 ± 0.0	0.032 ± 0.006	0.005 ± 0.0	0.032 ± 0.006	0.916 ± 0.0
ResNet-56 ERM	0.039 ± 0.013	0.094 ± 0.009	0.039 ± 0.013	0.094 ± 0.009	0.867 ± 0.001
ResNet-56 HKRR	0.015 ± 0.001	0.059 ± 0.01	0.015 ± 0.001	0.047 ± 0.005	0.848 ± 0.004
ResNet-56 HJZ	0.013 ± 0.005	0.081 ± 0.012	0.014 ± 0.005	0.081 ± 0.012	0.863 ± 0.002
ResNet-56 Isotonic	0.005 ± 0.001	0.079 ± 0.009	0.007 ± 0.0	0.078 ± 0.008	0.863 ± 0.002

Figure 4: **Top**: Test accuracy vs. maximum group-wise calibration error (smECE) averaged over three train/validation splits for ViT and DenseNet on Camelyon17. Multicalibration post-processing has scope for improvement in both settings, and does so with limited loss in accuracy. **Bottom**: Impact of multicalibration post-processing algorithms for Civil Comments (DistilBERT) and Amazon Polarity (ResNet-56). Multicalibration post-processing and isotonic calibration both offer improvements to worst group calibration error.

multicalibration on tabular data. Isotonic regression also directly improves worst group calibration error over ERM in 4/6 of our experiments on larger models (see, e.g., Figures 4, G.2). Due to the fact that it is efficient and parameter free, we do not see a downside to running Isotonic regression (or any other calibration method) and testing if the maximum group-wise calibration error is beneath a desired threshold.

5.1 Limitations and Conclusion

One limitation of our results on language and vision datasets — as opposed to the tabular datasets — is that we do not optimize for the best choice of base model hyperparameters on each separate calibration split (e.g. changing learning rate or batch size between calibration fractions 0.2 and 0.4). In practice, we imagine that a practitioner would first fit the best possible ERM hyperparameters without using any holdout calibration data. Subsequently, they would then experiment with modifying the amount of hold out data to feed to multicalibration. We choose our hyperparameters for our base model to reflect this particular tuning strategy.

Another limitation of our results is that they are restricted to binary classification problems. While multicalibration algorithms do extend to multiclass problems, this extension comes at a severe cost of sample efficiency usually *exponential* in the number of labels (Zhao et al., 2021). We show that — at least for tabular datasets — current multicalibration algorithms do not significantly improve upon a competitive ERM. If we were to further burden the multicalibration algorithm with the larger sample complexity of an additional label, we do not expect that their performance will improve. Nonetheless, we plan to investigate the multiclass setting in future work, and believe that those findings will be consistent with the results present in this paper.

We believe that our work illuminates many avenues towards improving the viability of multicalibration algorithms in practice. For example, developing parameter free multicalibration methods (akin to what smECE accomplishes for calibration metrics) is an important direction with direct impacts on the practice of fair machine learning. Similarly, post-processing techniques with better empirical sample complexity could significantly help the practice of multicalibration.

Acknowledgements. SD was supported by the Department of Defense through the National Defense Science & Engineering Graduate (NDSEG) Fellowship Program. This work was also supported by NSF CAREER Award CCF-2239265 and an Amazon Research Award. Any opinions, findings, and conclusions or recommendations expressed in this material are those of the author(s) and do not reflect the views of sponsors such as Amazon or NSF. The authors would like to thank Bhavya Vasudeva for discussions that were helpful in the design of early experiments, and Eric Zhao for help in utilizing the HJZ algorithms.

References

- Bándi, P., Geessink, O., Manson, Q., Dijk, M. V., Balkenhol, M., Hermsen, M., Bejnordi, B. E., Lee, B., Paeng, K., Zhong, A., Li, Q., Zanjani, F. G., Zinger, S., Fukuta, K., Komura, D., Ovtcharov, V., Cheng, S., Zeng, S., Thagaard, J., Dahl, A. B., Lin, H., Chen, H., Jacobsson, L., Hedlund, M., Çetin, M., Halici, E., Jackson, H., Chen, R., Both, F., Franke, J., Küsters-Vandeveld, H., Vreuls, W., Bult, P., van Ginneken, B., van der Laak, J., and Litjens, G. (2019). From detection of individual metastases to classification of lymph node status at the patient level: The CAMELYON17 challenge. *IEEE Trans. Medical Imaging*, 38(2):550–560. [17](#)
- Barda, N., Riesel, D., Akriv, A., Levy, J., Finkel, U., Yona, G., Greenfeld, D., Sheiba, S., Somer, J., Bachmat, E., et al. (2020). Developing a covid-19 mortality risk prediction model when individual-level data are not available. *Nature communications*, 11(1):4439. [2](#)
- Barda, N., Yona, G., Rothblum, G. N., Greenland, P., Leibowitz, M., Balicer, R., Bachmat, E., and Dagan, N. (2021). Addressing bias in prediction models by improving subpopulation calibration. *Journal of the American Medical Informatics Association*, 28(3):549–558. [4, 6](#)
- Barenstein, M. (2019). Propublica’s compas data revisited. *arXiv preprint arXiv:1906.04711*. [6](#)
- Bastani, O., Gupta, V., Jung, C., Noarov, G., Ramalingam, R., and Roth, A. (2022). Practical adversarial multivalid conformal prediction. *Advances in Neural Information Processing Systems*, 35:29362–29373. [2](#)
- Becker, B. and Kohavi, R. (1996). Adult. UCI Machine Learning Repository. DOI: <https://doi.org/10.24432/C5XW20>. [16](#)
- Benz, N. C. and Rodriguez, M. (2023). Human-aligned calibration for ai-assisted decision making. In *NeurIPS*. [15](#)
- Bequé, A., Coussement, K., Gayler, R., and Lessmann, S. (2017). Approaches for credit scorecard calibration: An empirical analysis. *Knowledge-Based Systems*, 134:213–227. [1](#)
- Blasiok, J., Gopalan, P., Hu, L., and Nakkiran, P. (2023). A unifying theory of distance from calibration. In *Proceedings of the 55th Annual ACM Symposium on Theory of Computing*. [4, 5](#)
- Borkan, D., Dixon, L., Sorensen, J., Thain, N., and Vasserman, L. (2019). Nuanced metrics for measuring unintended bias with real data for text classification. In *WWW (Companion Volume)*, pages 491–500. ACM. [17](#)
- Blasiok, J., Gopalan, P., Hu, L., Kalai, A. T., and Nakkiran, P. (2024). Loss minimization yields multicalibration for large neural networks. In *Innovations in Theoretical Computer Science*. [4](#)
- Blasiok, J., Gopalan, P., Hu, L., and Nakkiran, P. (2023). When does optimizing a proper loss yield calibration? In *Advances in Neural Information Processing Systems*. [2, 4](#)
- Blasiok, J. and Nakkiran, P. (2023). Smooth ece: Principled reliability diagrams via kernel smoothing. [4, 5](#)
- Carrell, A. M., Mallinar, N., Lucas, J., and Nakkiran, P. (2022). The calibration generalization gap. [6, 15](#)
- Chen, R. J., Wang, J. J., Williamson, D. F., Chen, T. Y., Lipkova, J., Lu, M. Y., Sahai, S., and Mahmood, F. (2023). Algorithmic fairness in artificial intelligence for medicine and healthcare. *Nature biomedical engineering*, 7(6):719–742. [2](#)

- Chouldechova, A. (2017). Fair prediction with disparate impact: A study of bias in recidivism prediction instruments. *Big data*, 5(2):153–163. [1](#)
- Cleary, T. A. (1968). Test bias: Prediction of grades of negro and white students in integrated colleges. *Journal of Educational Measurement*, 5(2):115–124. [1](#)
- Cooper, A. F., Barocas, S., Sa, C. D., and Sen, S. (2023). Variance, Self-Consistency, and Arbitrariness in Fair Classification. [16](#)
- Dahabreh, I. J., Chan, J. A., Earley, A., Moorthy, D., Avendano, E. E., Trikalinos, T. A., Balk, E. M., and Wong, J. B. (2017). A review of validation and calibration methods for health care modeling and simulation. *Modeling and Simulation in the Context of Health Technology Assessment: Review of Existing Guidance, Future Research Needs, and Validity Assessment [Internet]*. [1](#)
- Detommaso, G., Bertran, M., Fogliato, R., and Roth, A. (2024). Multicalibration for confidence scoring in llms. In *International Conference on Machine Learning*. [4](#), [5](#), [15](#), [16](#)
- Devic, S., Korolova, A., Kempe, D., and Sharan, V. (2024). Stability and multigroup fairness in ranking with uncertain predictions. In *International Conference on Machine Learning*. [2](#)
- Ding, F., Hardt, M., Miller, J., and Schmidt, L. (2021). Retiring adult: New datasets for fair machine learning. In *Advances in Neural Information Processing Systems*, pages 6478–6490. [16](#)
- Dosovitskiy, A., Beyer, L., Kolesnikov, A., Weissenborn, D., Zhai, X., Unterthiner, T., Dehghani, M., Minderer, M., Heigold, G., Gelly, S., Uszkoreit, J., and Houshy, N. (2021). An image is worth 16x16 words: Transformers for image recognition at scale. In *ICLR OpenReview.net*. [9](#), [24](#)
- Duchene, C., Jamet, H., Guillaume, P., and Dehak, R. (2023). A benchmark for toxic comment classification on civil comments dataset. *CoRR*, abs/2301.11125. [8](#), [24](#)
- Dwork, C., Kim, M. P., Reingold, O., Rothblum, G. N., and Yona, G. (2021). Outcome indistinguishability. In *Proceedings of the 53rd Annual ACM SIGACT Symposium on Theory of Computing*, pages 1095–1108. [2](#)
- Dwork, C., Lee, D., Lin, H., and Tankala, P. (2023). From pseudorandomness to multi-group fairness and back. In *The Thirty Sixth Annual Conference on Learning Theory*, pages 3566–3614. PMLR. [2](#)
- Federal Financial Institutions Examination Council (2017). HMDA Data Publication. Released due to the Home Mortgage Disclosure Act. [16](#)
- Globus-Harris, I., Gupta, V., Jung, C., Kearns, M., Morgenstern, J., and Roth, A. (2023). Multicalibrated regression for downstream fairness. In *Proceedings of the 2023 AAAI/ACM Conference on AI, Ethics, and Society*, pages 259–286. [15](#)
- Gollakota, A., Gopalan, P., Klivans, A., and Stavropoulos, K. (2024). Agnostically learning single-index models using omnipredictors. In *Advances in Neural Information Processing Systems*, volume 36. [2](#)
- Gopalan, P., Hu, L., Kim, M. P., Reingold, O., and Wieder, U. (2023). Loss minimization through the lens of outcome indistinguishability. In *Innovations in Theoretical Computer Science*. [2](#)
- Gopalan, P., Kalai, A. T., Reingold, O., Sharan, V., and Wieder, U. (2022a). Omnipredictors. In *Innovations in Theoretical Computer Science*. [2](#)
- Gopalan, P., Kim, M. P., Singhal, M. A., and Zhao, S. (2022b). Low-degree multicalibration. In *Conference on Learning Theory*, pages 3193–3234. PMLR. [2](#), [5](#)
- Gopalan, P., Reingold, O., Sharan, V., and Wieder, U. (2022c). Multicalibrated partitions for importance weights. In *International Conference on Algorithmic Learning Theory*, pages 408–435. PMLR. [2](#)
- Guo, C., Pleiss, G., Sun, Y., and Weinberger, K. Q. (2017). On calibration of modern neural networks. In *International conference on machine learning*, pages 1321–1330. PMLR. [1](#), [4](#), [5](#), [15](#)
- Haghtalab, N., Jordan, M., and Zhao, E. (2023). A unifying perspective on multi-calibration: Game dynamics for multi-objective learning. In *Advances in Neural Information Processing Systems*, volume 36. [2](#), [3](#), [4](#), [5](#), [22](#), [23](#)

- He, K., Zhang, X., Ren, S., and Sun, J. (2016). Deep residual learning for image recognition. In *CVPR*, pages 770–778. IEEE Computer Society. [24](#)
- Hébert-Johnson, U., Kim, M., Reingold, O., and Rothblum, G. (2018). Multicalibration: Calibration for the (computationally-identifiable) masses. In *International Conference on Machine Learning*, pages 1939–1948. PMLR. [2](#), [3](#), [4](#), [5](#), [22](#)
- Huang, G., Liu, Z., van der Maaten, L., and Weinberger, K. Q. (2017). Densely connected convolutional networks. In *CVPR*, pages 2261–2269. IEEE Computer Society. [24](#)
- Jung, C., Lee, C., Pai, M., Roth, A., and Vohra, R. (2021). Moment multicalibration for uncertainty estimation. In *Conference on Learning Theory*, pages 2634–2678. PMLR. [2](#)
- Jung, C., Noarov, G., Ramalingam, R., and Roth, A. (2023). Batch multivalid conformal prediction. In *International Conference on Learning Representations*. [2](#)
- Kim, M. P., Kern, C., Goldwasser, S., Kreuter, F., and Reingold, O. (2022). Universal adaptability: Target-independent inference that competes with propensity scoring. *Proceedings of the National Academy of Sciences*, 119(4):e2108097119. [2](#)
- Kirichenko, P., Izmailov, P., and Wilson, A. G. (2023). Last layer re-training is sufficient for robustness to spurious correlations. In *The Eleventh International Conference on Learning Representations, ICLR 2023, Kigali, Rwanda, May 1-5, 2023*. OpenReview.net. [15](#)
- Kleinberg, J., Mullainathan, S., and Raghavan, M. (2017). Inherent trade-offs in the fair determination of risk scores. In *Innovations in Theoretical Computer Science*. [1](#)
- Koh, P. W., Sagawa, S., Marklund, H., Xie, S. M., Zhang, M., Balsubramani, A., Hu, W., Yasunaga, M., Phillips, R. L., Gao, I., Lee, T., David, E., Stavness, I., Guo, W., Earnshaw, B., Haque, I. S., Beery, S. M., Leskovec, J., Kundaje, A., Pierson, E., Levine, S., Finn, C., and Liang, P. (2021). WILDS: A benchmark of in-the-wild distribution shifts. In *ICML*, volume 139 of *Proceedings of Machine Learning Research*, pages 5637–5664. PMLR. [17](#)
- Kumar, A., Sarawagi, S., and Jain, U. (2018). Trainable calibration measures for neural networks from kernel mean embeddings. In *International Conference on Machine Learning*, pages 2805–2814. PMLR. [15](#)
- La Cava, W., Lett, E., and Wan, G. (2022). Proportional multicalibration. *arXiv preprint arXiv:2209.14613*. [4](#)
- La Cava, W. G., Lett, E., and Wan, G. (2023). Fair admission risk prediction with proportional multicalibration. In *Conference on Health, Inference, and Learning*, pages 350–378. PMLR. [2](#)
- LaBonte, T., Muthukumar, V., and Kumar, A. (2023). Towards last-layer retraining for group robustness with fewer annotations. In *NeurIPS*. [15](#)
- Liu, L. T., Simchowitz, M., and Hardt, M. (2019). The implicit fairness criterion of unconstrained learning. In *International Conference on Machine Learning*, pages 4051–4060. PMLR. [2](#), [4](#)
- Liu, Z., Luo, P., Wang, X., and Tang, X. (2015). Deep learning face attributes in the wild. In *Proceedings of International Conference on Computer Vision (ICCV)*. [16](#)
- Mao, Y., Deng, Z., Yao, H., Ye, T., Kawaguchi, K., and Zou, J. (2023). Last-layer fairness fine-tuning is simple and effective for neural networks. *CoRR*, abs/2304.03935. [15](#)
- Minderer, M., Djolonga, J., Romijnders, R., Hubis, F., Zhai, X., Houlsby, N., Tran, D., and Lucic, M. (2021). Revisiting the calibration of modern neural networks. In *Advances in Neural Information Processing Systems*, volume 34, pages 15682–15694. [1](#), [15](#)
- Moro, S., Rita, P., and Cortez, P. (2012). Bank Marketing. UCI Machine Learning Repository. DOI: <https://doi.org/10.24432/C5K306>. [16](#)
- Niculescu-Mizil, A. and Caruana, R. (2005). Predicting good probabilities with supervised learning. In *International Conference on Machine Learning*, pages 625–632. [1](#)
- Obermeyer, Z., Powers, B., Vogeli, C., and Mullainathan, S. (2019). Dissecting racial bias in an algorithm used to manage the health of populations. *Science*, 366(6464):447–453. [1](#), [6](#)

- Ovalle, A., Subramonian, A., Gautam, V., Gee, G., and Chang, K.-W. (2023). Factoring the matrix of domination: A critical review and reimagining of intersectionality in ai fairness. In *Proceedings of the 2023 AAAI/ACM Conference on AI, Ethics, and Society*, pages 496–511. 5
- Pennington, J., Socher, R., and Manning, C. D. (2014). Glove: Global vectors for word representation. In *EMNLP*, pages 1532–1543. ACL. 24
- Perez-Lebel, A., Morvan, M. L., and Varoquaux, G. (2023). Beyond calibration: estimating the grouping loss of modern neural networks. In *International Conference on Learning Representations*. 15
- Pfohl, S. R., Zhang, H., Xu, Y., Foryciarz, A., Ghassemi, M., and Shah, N. H. (2022). A comparison of approaches to improve worst-case predictive model performance over patient subpopulations. *Scientific reports*, 12(1):3254. 4
- Platt, J. et al. (1999). Probabilistic outputs for support vector machines and comparisons to regularized likelihood methods. *Advances in large margin classifiers*, 10(3):61–74. 1, 5
- Sagawa, S., Koh, P. W., Hashimoto, T. B., and Liang, P. (2019). Distributionally robust neural networks for group shifts: On the importance of regularization for worst-case generalization. *CoRR*, abs/1911.08731. 16
- Sahlgren, O. and Laitinen, A. (2020). Algorithmic fairness and its limits in group-formation. In *Tethics: Conference on Technology Ethics*, pages 38–54. 4
- Sanh, V., Debut, L., Chaumond, J., and Wolf, T. (2019). Distilbert, a distilled version of BERT: smaller, faster, cheaper and lighter. *CoRR*, abs/1910.01108. 9, 24
- Shabat, E., Cohen, L., and Mansour, Y. (2020). Sample complexity of uniform convergence for multicalibration. In *Advances in Neural Information Processing Systems*, volume 33, pages 13331–13340. 2, 4
- Shalev-Shwartz, S. and Ben-David, S. (2014). *Understanding machine learning: From theory to algorithms*. Cambridge university press. 4
- Sharma, S., Gee, A. H., Paydarfar, D., and Ghosh, J. (2021). Fair-n: Fair and robust neural networks for structured data. In *AIES*, pages 946–955. ACM. 16
- Wang, C. (2023). Calibration in deep learning: A survey of the state-of-the-art. *arXiv preprint arXiv:2308.01222*. 15
- Yeh, I.-C. (2016). Default of Credit Card Clients. UCI Machine Learning Repository. DOI: <https://doi.org/10.24432/C55S3H>. 16
- Yuksekgonul, M., Zhang, L., Zou, J. Y., and Guestrin, C. (2024). Beyond confidence: Reliable models should also consider atypicality. In *Advances in Neural Information Processing Systems*, volume 36. 15
- Zadrozny, B. and Elkan, C. (2002). Transforming classifier scores into accurate multiclass probability estimates. In *Proceedings of the eighth ACM SIGKDD international conference on Knowledge discovery and data mining*, pages 694–699. 5, 6
- Zhang, L., Roth, A., and Zhang, L. (2024). Fair risk control: A generalized framework for calibrating multi-group fairness risks. In *International Conference on Machine Learning*. 15
- Zhang, X., Zhao, J. J., and LeCun, Y. (2015). Character-level convolutional networks for text classification. In *NIPS*, pages 649–657. 17
- Zhao, S., Kim, M., Sahoo, R., Ma, T., and Ermon, S. (2021). Calibrating predictions to decisions: A novel approach to multi-class calibration. *Advances in Neural Information Processing Systems*, 34:22313–22324. 10

A Additional Related Work

Limitations of Calibration. A collection of works characterize the limitations of calibration as a property of predictors. Of particular note is [Perez-Lebel et al. \(2023\)](#), who remark that calibration is often misunderstood in the literature, as it does not guarantee that output probabilities are close to the ground truth probability distribution. We make no such claim about calibration, and only justify its use in order to ensure model predictions are meaningful. [Yuksekgonul et al. \(2024\)](#) draw connections between calibration and atypicality of certain examples, improving group wise-performance of NNs without subgroup annotations via what they term “atypicality-aware recalibration.”

Applications of Multicalibration. Beyond classification, [Globus-Harris et al. \(2023\)](#) introduce algorithms that post-process multicalibrated regression functions to satisfy a variety of fairness constraints, and present experiments using such algorithms on logistic regression and gradient-boosted decision trees. [Benz and Rodriguez \(2023\)](#) study predictive confidence in the setting of AI-assisted decision making; they show the existence of distributions under which a “rational” decision maker is unlikely to find an optimal policy using calibrated confidence values, and prove that multicalibration with respect to the decision maker’s preliminary confidence values is often sufficient for aversion of such issues. [Zhang et al. \(2024\)](#) also utilize a generalization of multicalibration to tackle interesting problems like de-biased text generation and false negative rate control.

Calibration of NNs. Literature on the calibration of neural networks (NNs) is very rich; see for example a treatment by [Wang \(2023\)](#). Most importantly, [Minderer et al. \(2021\)](#) have run comprehensive, large-scale experiments detailing the degree to which modern NNs are calibrated. Their results show that current state-of-the-art models appear to be nearly perfectly calibrated, and appear to remain so even in the presence of distribution shift. This is in somewhat striking contrast to the earlier results of [Guo et al. \(2017\)](#), which demonstrated the best models at time of their publication to be quite miscalibrated, and highlighted the need to further investigate calibration measures. Our focus in this work is instead on evaluating multicalibration of predictors on datasets over which we can naturally define a collection of protected subgroups.

[Carrell et al. \(2022\)](#) examine a connection between generalization and *calibration generalization*, the difference in calibration error on train and test sets. In particular, they claim DNNs to be well-calibrated on their training sets and the accuracy generalization gap to upper bound the calibration generalization gap. Such observations imply NNs that generalize well to be well-calibrated.

Trainable Calibration Measures. Laplace Kernel calibration measures have been shown to be effective in enforcing confidence calibration for neural networks when used in training. In particular, using MMCE (Maximum Mean Calibration Error) as a regularizer in tandem with cross-entropy loss yields high accuracy predictions while moderately improving calibration by taming overconfident predictions ([Kumar et al., 2018](#)). Additionally, this metric is efficiently computable in quadratic time.

Subgroup Robustness. Several works in subgroup robustness literature examine the performance of NNs by *worst-group-accuracy*, particularly in cases where NNs tend to rely on spurious correlations. Recent works by [Kirichenko et al. \(2023\)](#); [LaBonte et al. \(2023\)](#) propose last-layer fine-tuning as a simple and computationally inexpensive way to do exactly that. Indeed, [Mao et al. \(2023\)](#) extend the method to address fairness concerns, appending a fairness constraint to the training objective during fine-tuning. Such works examine only one sensitive attribute at a time, and often consider the disjoint groups produced by unique values of this attribute in conjunction with label.

A.1 Equivalence of Early Stopping and Hyperparameter Sweeps

[Detommaso et al. \(2024\)](#) utilize two early-stopping criterion. The first is to halt further multicalibration iterations once the group conditioned on the bin set becomes “too small.” We also utilize this technique, which is inherent in the algorithm of HKRR. [Detommaso et al. \(2024\)](#) also use a holdout validation set to early-stop a variant of HKRR when the mean-squared error (MSE) on the hold-out set fails to decrease. We instead vary the permitted violation parameter α of HKRR, and select the best parameter with a holdout validation set. α controls the permitted calibration error conditioned on a group and particular bin (of width $\lambda = 0.1$ in our work). We believe that early stopping for a validation metric should have similar performance to running the full HKRR with a variety of α levels, and selecting

based on validation performance. Nonetheless, we note that in our experiments, we select based on validation smoothECE multicalibration error, while [Detommaso et al. \(2024\)](#) select on validation MSE. This could potentially lead to performance differences.

B Broader Impacts

Our work performs a comprehensive empirical evaluation of multicalibration post-processing, which could help practitioners apply these notions more effectively in practice. We note however, that fairness can be subtle, and multicalibration by itself may not be enough to ensure fairness. By now it is well understood that there are tradeoffs between different notions of fairness, and the right definitions to be deployed are context-dependent and depend on societal norms. Therefore, our results on the latent multicalibration of neural networks should not be construed as implying that these models are already fair, and care should be taken before deploying any ML model in applications with consequential societal outcomes.

C Dataset and Subgroup Descriptions

Here, we detail the datasets and group information used in all experiments.

C.1 Tabular Datasets

The ACS Income dataset, introduced by [Ding et al. \(2021\)](#), is a superset of the UCI Adult⁴ dataset ([Becker and Kohavi, 1996](#)) derived from additional US Census data. We use the `folktables` package introduced alongside the work. In particular, we consider the task of predicting whether an American adult living in California receives income greater than \$50,000 in the year 2018. Features include race, gender, age, and occupation. For this task, the dataset furnishes just under 200,000 samples.

The UCI Bank Marketing dataset documents 45,000 phone calls made by a Portuguese banking institution over the course of several marketing campaigns ([Moro et al., 2012](#)). We consider the task of predicting whether, on a given call, the client will subscribe a term deposit, given features characterizing the housing, occupation, education, and age of the client.

The UCI Default of Credit Card Clients dataset (termed “Credit Default” in our experiments) documents the partial credit histories of 30,000 Taiwanese individuals ([Yeh, 2016](#)). We consider the task of predicting whether an individual will default on credit card debt, given payment history and additional identity attributes.

The HMDA (Home Mortgage Disclosure Act) dataset documents the US mortgage applications, identity attributes of associated applicants, and the outcome of these applications ([Federal Financial Institutions Examination Council, 2017](#)). We use a 114,000-sample variant of this dataset given by [Cooper et al. \(2023\)](#), and consider the task of predicting whether a 2017 application in the state of Texas was accepted.

The MEPS (Medical Expenditure Panel Survey) dataset comes from the US Department of Health and Human Services and documents healthcare utilization of US households. We use a 11,000-sample variant of the dataset, originally studied in [Sharma et al. \(2021\)](#), and consider the task of predicting whether a household makes at least 10 medical visits, given socioeconomic and geographic information of household applicants.

C.2 Image Datasets

The CelebA dataset, introduced by [Liu et al. \(2015\)](#), consists of 200,000 cropped and aligned images of celebrity faces. We consider the task of predicting hair color, a task known to be difficult for certain label-dependent subgroups due to the existence of spurious correlations ([Sagawa et al., 2019](#)). Metadata documents certain characteristics of the individuals in the images such as gender, face shape, hair style, and the presence of fashion accessories.

⁴For comparison with prior work, we include the original UCI Adult dataset in our benchmark repository.

The Camelyon17 dataset, introduced by [Bánda et al. \(2019\)](#), consists of histopathological images of human lymph node tissue. We use a patch-based variant of this dataset, introduced by [Koh et al. \(2021\)](#), which consists of 450,000 96x96 images. Unlike [Koh et al. \(2021\)](#), we shuffle the predetermined training and test splits. We consider the task of predicting whether a given image contains tumorous tissue. Metadata documents the hospital from which a given patch originates, and the original slide from which the patch is drawn.

C.3 Language Datasets

The CivilComments dataset, introduced by [Borkan et al. \(2019\)](#), contains 450,000 online comments annotated for toxicity and identity mentions by crowdsourcing and majority vote. We use the WILDS variant of this dataset, provided by [Koh et al. \(2021\)](#), though we shuffle the predetermined training and test splits, and consider the task of prediction whether a given comment is labeled toxic.

The Amazon Polarity dataset, also introduced by [Zhang et al. \(2015\)](#) and a subset of the Amazon Reviews dataset, provides the text content of 4,000,000 Amazon reviews. A review receives the label 1 when associated with a rating greater than or equal to 4 stars, and a label of 0 when associated with a rating of less than or equal to 2 stars. As with Yelp Polarity, this dataset comes with no metadata, so we define groups based on the presence of meaningful words. We use a randomly-drawn, 400,000 sample subset across all experiments.

C.4 Groups for Tabular Datasets

Here we present the subgroups considered for each dataset in our experiments. In all cases, we only consider subgroups composing at least a 0.005-fraction of the underlying dataset.

Note that the ‘Dataset’ row in each table does not correspond to a group used in multicalibration post-processing, nor are aggregate metrics used to compute worst-group metrics such as max smECE. We include this row for convenience.

group name	n samples	fraction	y mean
Black Adults	8508	0.0435	0.3461
Black Females	4353	0.0222	0.3193
Women	92354	0.4720	0.3491
Never Married	68408	0.3496	0.2344
American Indian	1294	0.0066	0.2836
Seniors	14476	0.0740	0.5410
White Women	55856	0.2855	0.3729
Multiracial	8206	0.0419	0.3572
Asian	32709	0.1672	0.4805
Dataset	195665	1.0000	0.4106

Figure 5: ACS Income groups.

group name	n samples	fraction	y mean
Job = Management	9458	0.2092	0.1376
Job = Technician	7597	0.1680	0.1106
Job = Entrepreneur	1487	0.0329	0.0827
Job = Blue-Collar	9732	0.2153	0.0727
Job = Retired	2264	0.0501	0.2279
Marital = Married	27214	0.6019	0.1012
Marital = Single	12790	0.2829	0.1495
Education = Primary	6851	0.1515	0.0863
Education = Secondary	23202	0.5132	0.1056
Education = Tertiary	13301	0.2942	0.1501
Housing = Yes	25130	0.5558	0.0770
Housing = No	20081	0.4442	0.1670
Age < 30	3050	0.0675	0.1951
30 ≤ Age < 40	17359	0.3840	0.1129
Age ≥ 50	12185	0.2695	0.1287
Dataset	45211	1.0000	0.1170

Figure 6: Bank Marketing groups.

group name	n samples	fraction	y mean
Male, Age < 30	3281	0.1094	0.2405
Single	15964	0.5321	0.2093
Single, Age > 30	6888	0.2296	0.1992
Female	18112	0.6037	0.2078
Married, Age < 30	1482	0.0494	0.2611
Married, Age > 60	225	0.0075	0.2667
Education = High School	4917	0.1639	0.2516
Education = High School, Married	2861	0.0954	0.2635
Education = High School, Age > 40	2456	0.0819	0.2577
Education = University, Age < 25	1610	0.0537	0.2795
Female, Education = University	8656	0.2885	0.2220
Education = Graduate School	10585	0.3528	0.1923
Female, Education = Graduate School	6231	0.2077	0.1814
Dataset	30000	1.0000	0.2212

Figure 7: Credit Default groups.

group name	n samples	fraction	y mean
Applicant Ethnicity: Hispanic or Latino	26416	0.2313	0.6806
Applicant Ethnicity: Not Hispanic or Latino	73527	0.6439	0.7940
Applicant Ethnicity: Not provided	14128	0.1237	0.6704
Applicant Sex: Female	32143	0.2815	0.7319
Applicant Sex: Male	72635	0.6361	0.7713
Co-Applicant Sex: Female	35164	0.3080	0.8029
Co-Applicant Sex: Male	10336	0.0905	0.7767
Applicant Race: Black	9044	0.0792	0.6703
Applicant Race: Asian	8086	0.0708	0.8097
Applicant Race: Native American or Alaskan	1019	0.0089	0.5927
Co-Applicant Race: Black	2760	0.0242	0.7120
Co-Applicant Race: Asian	3339	0.0292	0.8194
Dataset	114185	1.0000	0.7524

Figure 8: HMDA groups.

group name	n samples	fraction	y mean
Age 0-18	3308	0.2986	0.0605
Age 19-34	2468	0.2228	0.1021
Age 35-50	2186	0.1973	0.1404
Age 51-64	1813	0.1636	0.2670
Age 65-79	977	0.0882	0.4637
Not White	7121	0.6427	0.1227
Northeast	1553	0.1402	0.2260
Midwest	2020	0.1823	0.2040
South	4325	0.3904	0.1487
West	3181	0.2871	0.1481
Poverty Category 1	2435	0.2198	0.1577
Poverty Category 2	704	0.0635	0.1378
Poverty Category 3	1941	0.1752	0.1484
Poverty Category 4	3100	0.2798	0.1519
Dataset	11079	1.0000	0.1694

Figure 9: MEPS groups.

C.5 Groups for Image Datasets

group name	n samples	fraction	y mean
Male	84434	0.4168	0.0207
Female	118165	0.5832	0.2389
Arched Eyebrows	54090	0.2670	0.2227
Bangs	30709	0.1516	0.2310
Big Lips	48785	0.2408	0.1629
Chubby	11663	0.0576	0.0189
Double Chin	9459	0.0467	0.0248
Eyeglasses	13193	0.0651	0.0392
High Cheekbones	92189	0.4550	0.1949
Mouth Slightly Open	97942	0.4834	0.1737
Oval Face	57567	0.2841	0.1761
Pale Skin	8701	0.0429	0.2455
Receding Hairline	16163	0.0798	0.0630
Smiling	97669	0.4821	0.1812
Straight Hair	42222	0.2084	0.1518
Wavy Hair	64744	0.3196	0.2145
Wearing Hat	9818	0.0485	0.0168
Young	156734	0.7736	0.1581
Dataset	202599	1.0000	0.1480

Figure 10: CelebA groups.

group name	n samples	fraction	y mean
Hospital = 0	59436	0.1304	0.5000
Hospital = 1	34904	0.0766	0.5000
Hospital = 2	85054	0.1865	0.5000
Hospital = 3	129838	0.2848	0.5000
Hospital = 4	146722	0.3218	0.5000
Slide = 0	4316	0.0095	0.0083
Slide = 4	7294	0.0160	0.6697
Slide = 8	13455	0.0295	0.6469
Slide = 16	4971	0.0109	0.8236
Slide = 20	3810	0.0084	0.0071
Slide = 24	7727	0.0169	0.0238
Slide = 28	31878	0.0699	0.8469
Slide = 32	8831	0.0194	0.2466
Slide = 36	10661	0.0234	0.0015
Slide = 40	7395	0.0162	0.0170
Slide = 44	7958	0.0175	0.0030
Slide = 48	61110	0.1340	0.9273
Dataset	455954	1.0000	0.5000

Figure 11: Camelyon17 groups.

C.6 Groups for Language Datasets

group name	n samples	fraction	y mean
Male	20880	0.0466	0.1488
Female	33113	0.0739	0.1399
LGBTQ	14303	0.0319	0.2684
Not LGBTQ	433695	0.9681	0.1083
Christian	18961	0.0423	0.1103
Not Christian	380222	0.8487	0.1177
Muslim	13939	0.0311	0.2429
Not Muslim	418737	0.9347	0.1065
Other Religions	11030	0.0246	0.1528
Black	8448	0.0189	0.3638
Not Black	426444	0.9519	0.1049
White	14339	0.0320	0.3068
Not White	415090	0.9265	0.1016
Dataset	447998	1.0000	0.1134

Figure 12: Civil Comments groups.

group name	n samples	fraction	y mean
expensive	5834	0.0146	0.4434
cheap	10928	0.0273	0.2753
food	3868	0.0097	0.5476
health	2381	0.0060	0.6237
music	26463	0.0662	0.6192
book	108100	0.2703	0.5289
movie	36191	0.0905	0.4731
tech	8515	0.0213	0.4547
exercise	2262	0.0057	0.5535
garbage	3248	0.0081	0.0702
terrible	6138	0.0153	0.0893
incredible	2532	0.0063	0.7986
love	53005	0.1325	0.7212
again	26106	0.0653	0.4454
star	42632	0.1066	0.4495
Dataset	399980	1.0000	0.5009

Figure 13: Amazon Polarity groups.

C.7 Dataset Usage and Licensing

- **ACSIIncome**: While Folktables provides API for downloading ACS data, usage of this data is governed by the terms of use provided by the Census Bureau. For more information, see <https://www.census.gov/data/developers/about/terms-of-service.html>.
- **BankMarketing**: Creative Commons Attribution 4.0 International (CC BY 4.0)
- **CreditDefault**: Creative Commons Attribution 4.0 International (CC BY 4.0)
- **HMDA**: The variant we use is available for download on <https://github.com/pasta41/hmda?tab=readme-ov-file> under an MIT license.
- **MEPS**: The variant we use is available for download on <https://github.com/alangee/FaiR-N/tree/master> under an Apache 2.0 license.
- **Civil Comments**: This dataset is in the public domain and distributed under CC0.
- **Amazon Polarity**: We were not able to find a license for this dataset. It is a downstream variant of a dataset generated with content from Internet Archive⁵.
- **CelebA**: The creators of this dataset do not provide a license, though they encourage its use for non-commercial research purposes only.
- **Camelyon17**: This dataset is in the public domain and distributed under CC0.

D Hyperparameters for Multicalibration and Calibration Algorithms

Here, we detail the hyperparameters with which equip algorithms from Haghtalab et al. (2023) and Hébert-Johnson et al. (2018), as well as the hyperparameters used in standard calibration methods.

D.1 Hébert-Johnson et al. (2018) Algorithm

These authors do not report empirical performance of their algorithm. For consistency with calibration measures, we fix a bin width of $\lambda = 0.1$ in all experiments. The algorithm depends on one other hyperparameter α , which is some constant factor of the acceptable difference between mean prediction and mean label within each “category,” a subgroup $g \subseteq \mathcal{X}$ restricted to the preimage of a particular bin $b \subseteq [0, 1]$. Modulo the randomness induced by a statistical query oracle, this algorithm converges when violations within each category are sufficiently small. As originally proposed, we skip categories $g \cap f^{-1}(b)$ in iterations where $|g \cap f^{-1}(b)| \leq \lambda\alpha|g|$. For each dataset and each base predictor, we sweep over $\alpha \in \{0.1, 0.05, 0.025, 0.0125\}$.

D.2 Haghtalab et al. (2023) Algorithms

These authors present an empirical examination in conjunction with theoretical results, though our use of the algorithms differs significantly. Namely, instead of initializing predictions uniformly, we initialize with the predictions of some base predictor. The authors also train their multicalibration algorithms with substantially larger collections of subgroups, in some cases defining group by all unique values of individual features. Instead, we only consider a collection of at most 20 “protected” groups.

The authors evaluate six algorithms: four based on “no-regret best-response dynamics,” using an empirical risk minimizer as the adversary and Hedge, Prod, Optimistic Hedge, or Gradient Descent as the learner; two based on “no-regret no-regret dynamics,” using either Hedge or Optimistic Hedge as both the adversary and learner. On each task, and with each algorithm, the authors train for 50-100 iterations and sweep over learning rate decay rates of $\eta \in \{0.8, 0.85, 0.9, .95\}$ for the learner and, when applicable, rates of $\eta \in \{0.9, 0.95, 0.98, 0.99\}$ for the adversary. On two of the three datasets they examine, the authors fix a bin-width of $\lambda = 0.1$.

⁵http://archive.org/details/asin_listing/

In all experiments, we consider the same multicalibration algorithms but restrict to 30 iterations and a smaller collection of decay rates. In particular, for each dataset and base predictor, and for each of the six algorithms, we sweep over decay rates $\eta \in \{0.9, 0.95\}$ for the learner and $\eta \in \{0.9, 0.95, 0.98\}$ for the adversary. We justify these restrictions by noting that (1) our base predictors already achieve nontrivial accuracy on each task and (2) that this sweep covers a large portion of the optimal hyperparameters found in Haghtalab et al. (2023). For consistency with our hyperparameters for HKRR and chosen calibration measures, we fix $\lambda = 0.1$ on all datasets.

D.3 Temperature Implementation

Temperature scaling can be made hyperparameter-free by choosing a divisor T^* which minimizes the cross-entropy loss on a held-out calibration split. One can also fix T to some positive real number. For each dataset and base predictor, we examine both methods, scaling logits by $1/T$ for all $T \in \{0.2 \cdot k : k \in [20]\}$, as well as by $1/T^*$ with T^* obtained via the Pytorch implementation of L-BFGS. We report only the best temperature scaling method on a hold-out validation set.

E Models and Training

Here, we describe the models used as base predictors and their hyperparameters (or the procedure for obtaining these hyperparameters) in all experiments. Across all datasets, we use a train-validation-test split of (0.6 : 0.2 : 0.2), fixing the test set and determining train/validation sets via random seed. In all cases of a base-predictor hyperparameter search, we use validation accuracy to select hyperparameters.

E.1 Models Used on Tabular Data

On all tabular datasets, we examine five standard prediction models from supervised learning: Decision Tree, Random Forest, Logistic Regression, SVM, and Naive Bayes, using a Scikit-learn implementation in all cases. We also examine MLPs of varying architecture. For each dataset and prediction model, we examine all calibration fractions $CF \in \{0, 0.01, 0.05, 0.1, 0.2, 0.4, 0.6, 0.8, 1.0\}$. When $CF = 1.0$, we take the base predictor to output $1/2$ for all samples. During both hyperparameter search and test-set evaluation we average all metrics over five random splits of the training and validation data.

E.1.1 Standard Supervised Learning Models

For Decision Tree, we vary maximum depth over $\{\text{None}, 10, 20, 50\}$ and the minimum number of samples required to split an internal node over $\{2, 5, 10\}$. For Random Forest, we vary these same hyperparameters and fix the number of estimators at 100. For Logistic Regression and SVM, we vary regularization strength; for Logistic Regression we let the inverse regularization strength $C \in \{0.4, 1, 2, 4\}$ and for SVM we let the regularization strength $\alpha \in \{0.00001, 0.0001, 0.001, 0.01\}$. Naive Bayes is hyperparameter-free.

While Decision Tree, Random Forest, Logistic Regression, and Naive Bayes are naturally probabilistic, SVM is not. While Scikit-learn provides a probabilistic prediction method with the `predict_proba()` function, this is implemented via Platt scaling of the SVM scores. For this reason, we treat the SVM’s standard output labels as probabilities. For efficient on larger datasets, we also use the `SGDClassifier` implementation of SVM.

E.1.2 MLPs

To reduce computation during MLP hyperparameter search, for each dataset we constructed a smaller set of hyperparameters over which to sweep, based on what yielded the best performance in preliminary experiments. In what follows, we let a sequence $(\ell_i)_{i=1}^N$ denote the ordered layer widths for a particular MLP with N hidden layers. When we substitute some ℓ_i with BN, this indicates the presence of a batch-normalization layer. In all experiments with MLPs on tabular datasets, we use the Adam optimizer.

On ACS Income, we train for 50 epochs. We search over hidden-layer widths: (128, BN, 128), (128, 256, 128), and (128, BN, 256, BN, 128). We vary batch size over {32, 64, 128} and learning rate over {0.01, 0.001, 0.0001, 0.00001}.

On Bank Marketing, we train for 50 epochs. We search over hidden-layer widths of (100), (128, BN, 128), (128, 256, 128), and (128, BN, 256, BN, 128). We vary batch size over {64, 128, 256, 512} and learning rate over {0.001, 0.0001, 0.00001}. We also include a learning rate schedule under which our learning rate is 0.00005 for the first five epochs and 0.00001 for the remaining.

On Credit Default, we train for 5 epochs. We search over hidden-layer widths of (100), (128, 256, 128), and (128, BN, 256, BN, 128). We vary batch size over {16, 32, 64, 128} and learning rate over {0.01, 0.001, 0.0001, 0.00001}.

On HMDA, we train for 30 epochs. We search over hidden-layer widths of (100), (128, BN, 128), (128, 256, 128), and (128, BN, 256, BN, 128). We vary batch size over {128, 256, 512} and learning rate over {0.001, 0.0001, 0.00001}. We also include a learning rate schedule under which our learning rate is 0.00005 for the first five epochs and 0.00001 for the remaining. In addition, we search over weight decays in {0, 0.0001, 0.00001}.

On MEPS, we train for 50 epochs. We search over hidden-layer widths of (100), (128, BN, 128), (128, 256, 128), and (128, BN, 256, BN, 128). We vary batch size over {16, 32, 64} and learning rate over {0.1, 0.01, 0.01, 0.001, 0.0001, 0.00001}. In addition, we search over weight decays in {0, 0.0001, 0.00001}.

To ensure all NN outputs are probabilistic, we apply the softmax function before evaluating predictions or passing into any post-processing algorithm. The only exception to this rule is when we apply temperature scaling, which scales raw logits *before* passing into softmax.

E.2 Models Used on Vision and Language Tasks

On our vision and language datasets, we use much larger models, in some cases with as many as 85 million trainable parameters. We opt for hyperparameters already present in the literature, or alterations of such hyperparameters which give nontrivial accuracy, and we use the same hyperparameters for each calibration fraction. We examine all calibration fractions $CF \in \{0, 0.2, 0.4\}$ and average all runs over three random splits of the training and validation data.

Our experiments with language datasets involved two models: (1) DistilBERT, a pretrained transformer introduced by Sanh et al. (2019), and (2) a ResNet-56 using unfrozen, pretrained GloVe embeddings (Pennington et al., 2014), the implementation for which comes from Duchene et al. (2023).

On the CivilComments dataset, we train a DistilBERT for 10 epochs with a batch size of 16, learning rate of 0.00001, and weight decay of 0.01, using the Adam optimizer. We fix a maximum token length of 300.

On the Amazon Polarity dataset, we train a ResNet-56 with three input channels, which accept a stacked embedding of 512 dimensions. We use the `basic_english` tokenizer provided by `torchtext`, fixing a maximum token length of 70 and minimum frequency of 5. We train for 10 epochs with a batch size of 32 and learning rate of 0.0001 using Adam. Implementation-specific details are provided in our code.

Our experiments with vision datasets involve three models: (1) `vit-large-patch32-224-in21k`, a pretrained vision transformer introduced by Dosovitskiy et al. (2021), (2) ResNet-50 (He et al., 2016), and (3) DenseNet-121 (Huang et al., 2017).

On CelebA, we train the ViT for 10 epochs with a batch size of 64, learning rate of 0.0001, and weight decay of 0.01, using Adam. We also train a ResNet-50 for 50 epochs with a batch size of 64 and learning rate of 0.001, using SGD with a momentum of 0.9.

On Camelyon17, we train the ViT for 5 epochs with a batch size of 32, learning rate of 0.001, and weight decay of 0.01. We optimize with SGD, using a momentum of 0.9. We also train a DenseNet-121 for 10 epochs with a batch size of 32, learning rate of 0.001, and weight decay of 0.01, using SGD with a momentum of 0.9.

F Results on Tabular Datasets

F.1 Plots for All Multicalibration Algorithms

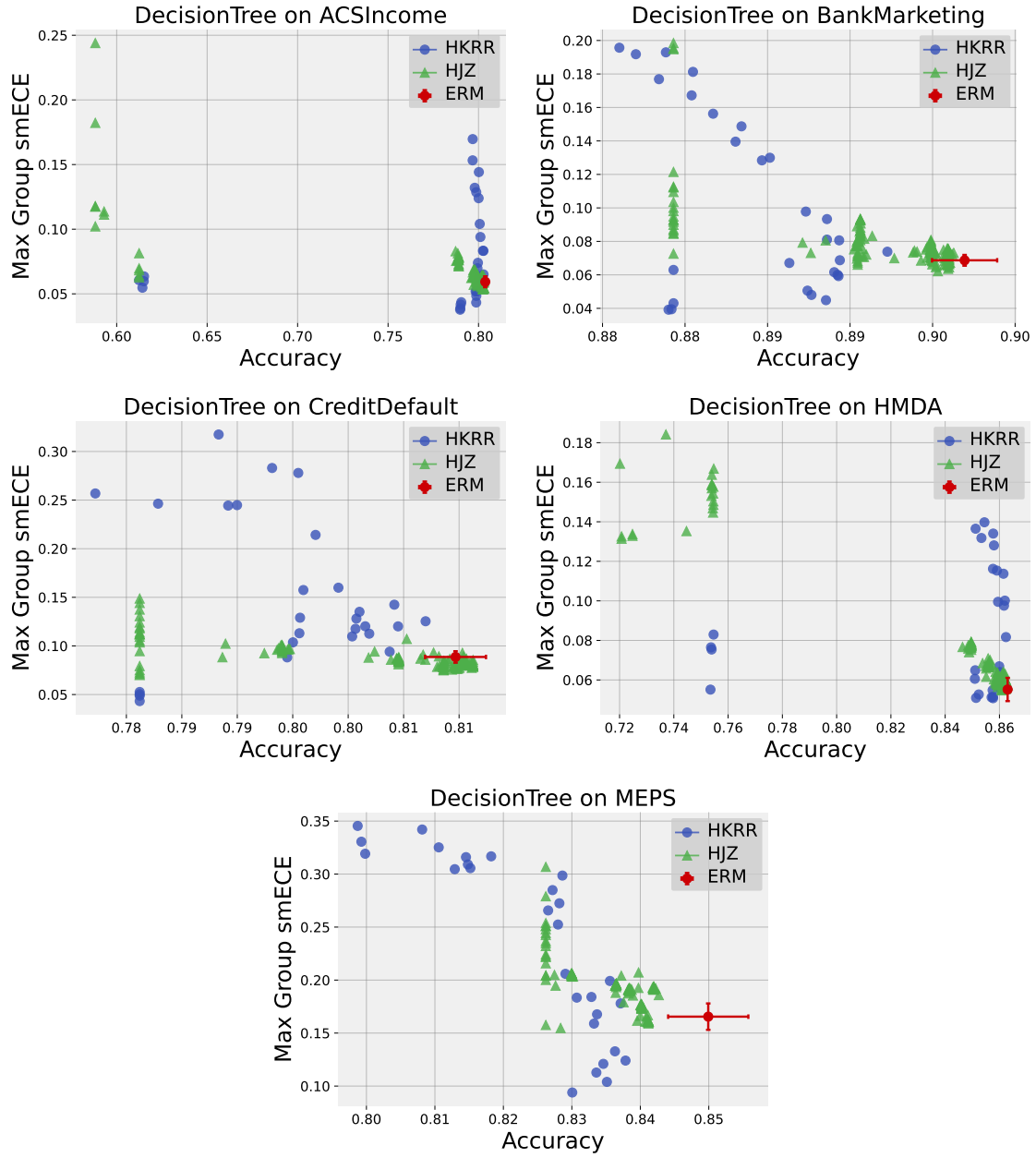


Figure 14: All multicalibration algorithms on Decision Trees.

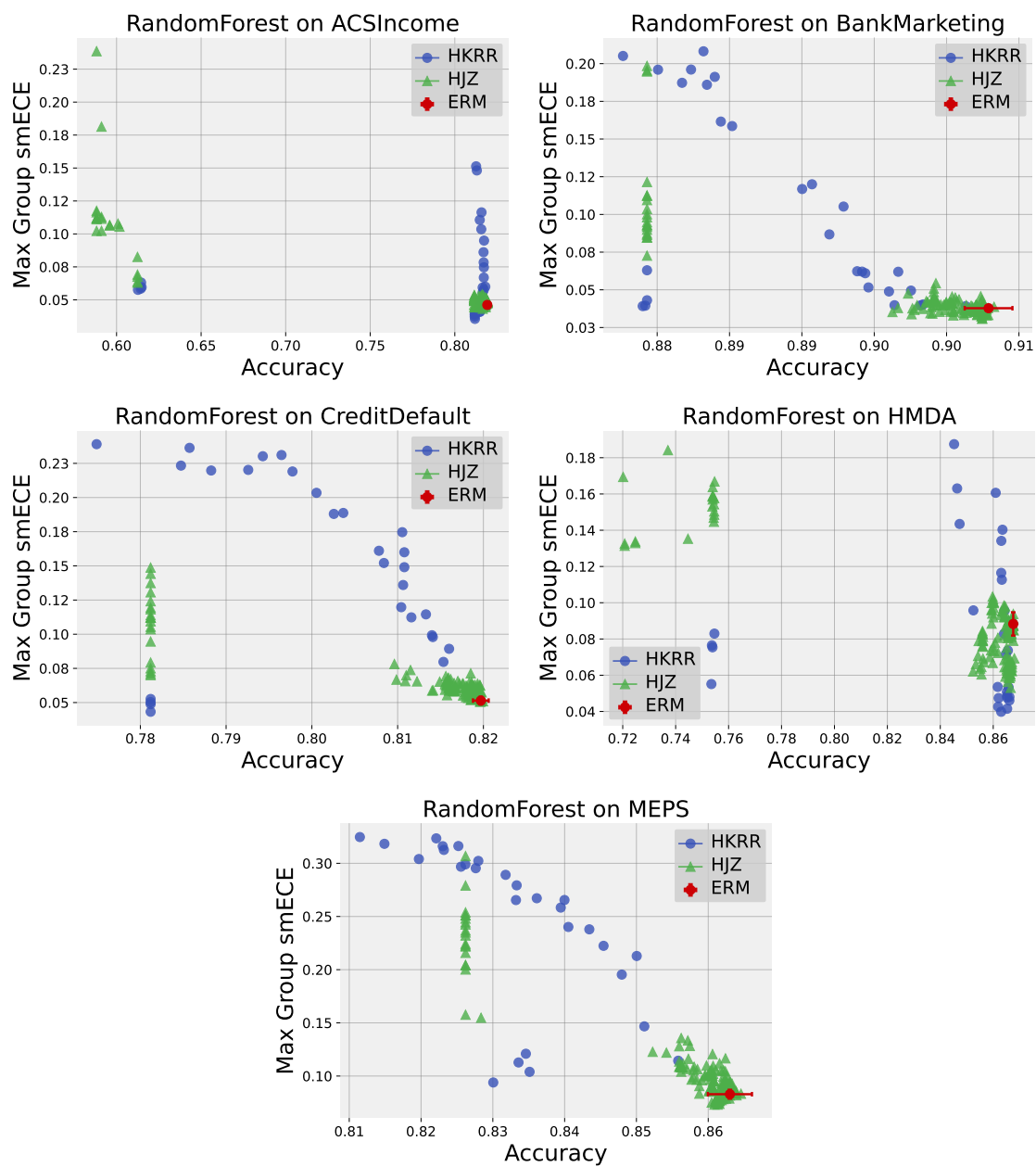


Figure 15: All multicalibration algorithms on Random Forest.

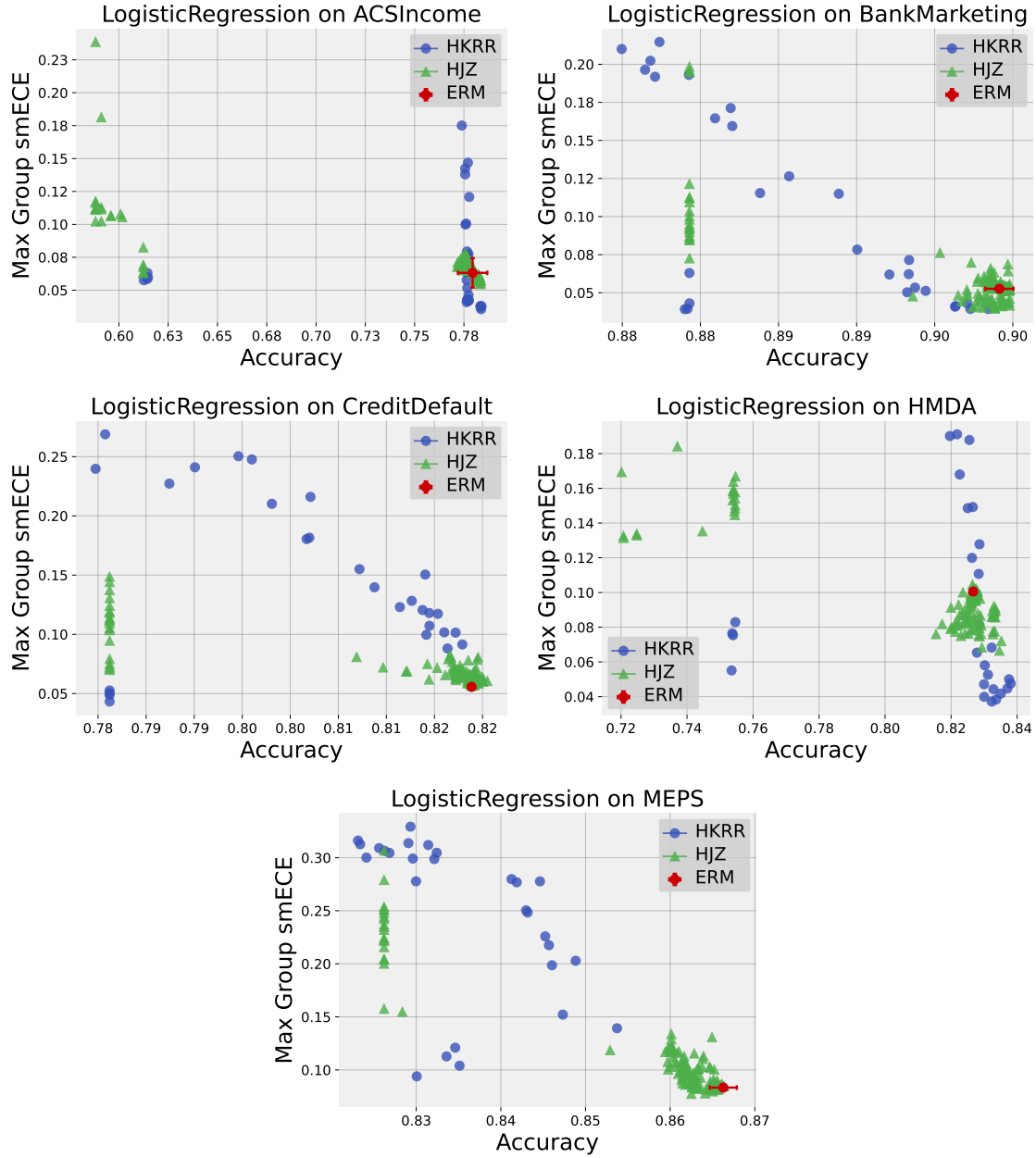


Figure 16: All multicalibration algorithms on Logistic Regression.

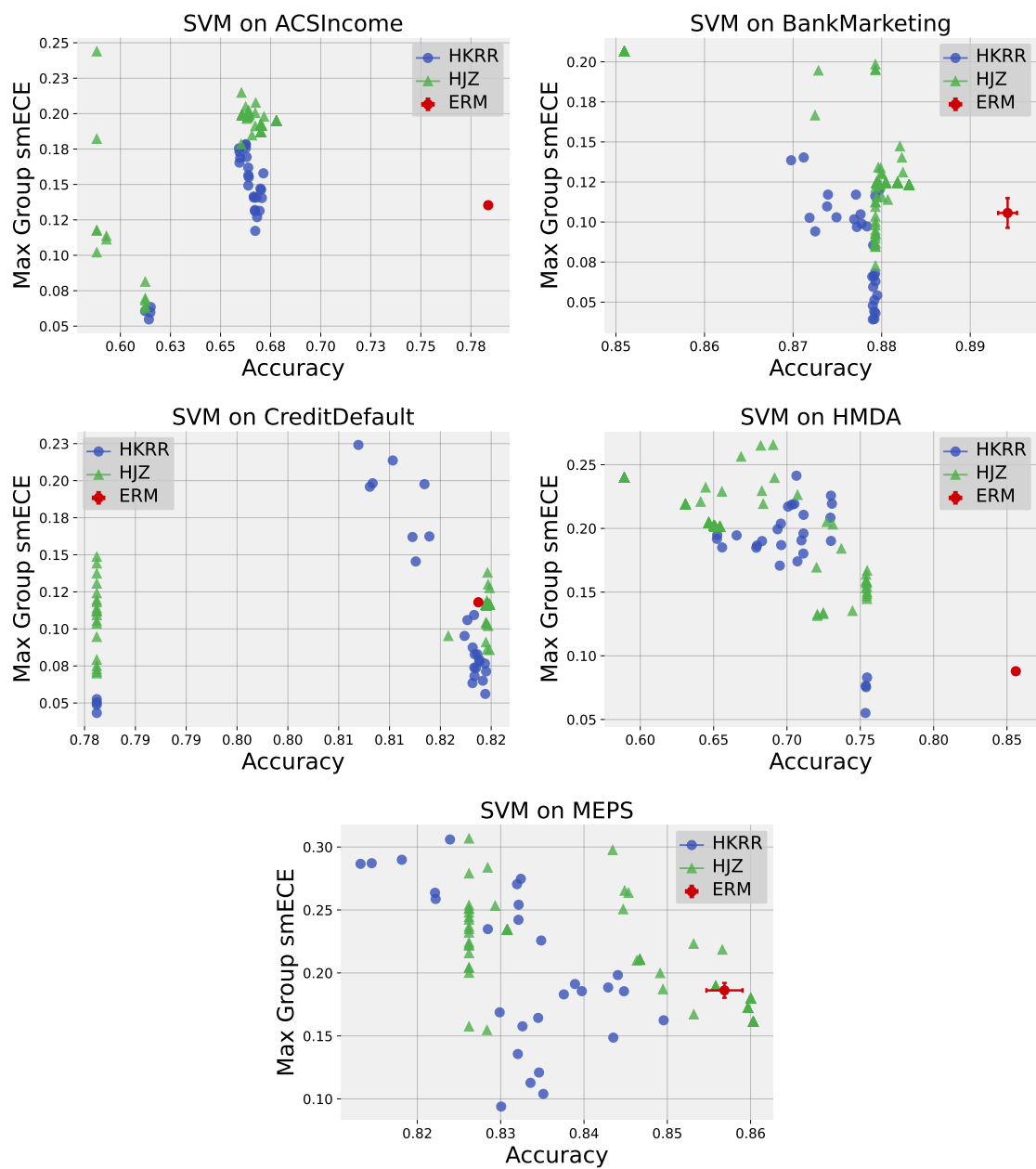


Figure 17: All multicalibration algorithms on SVMs.

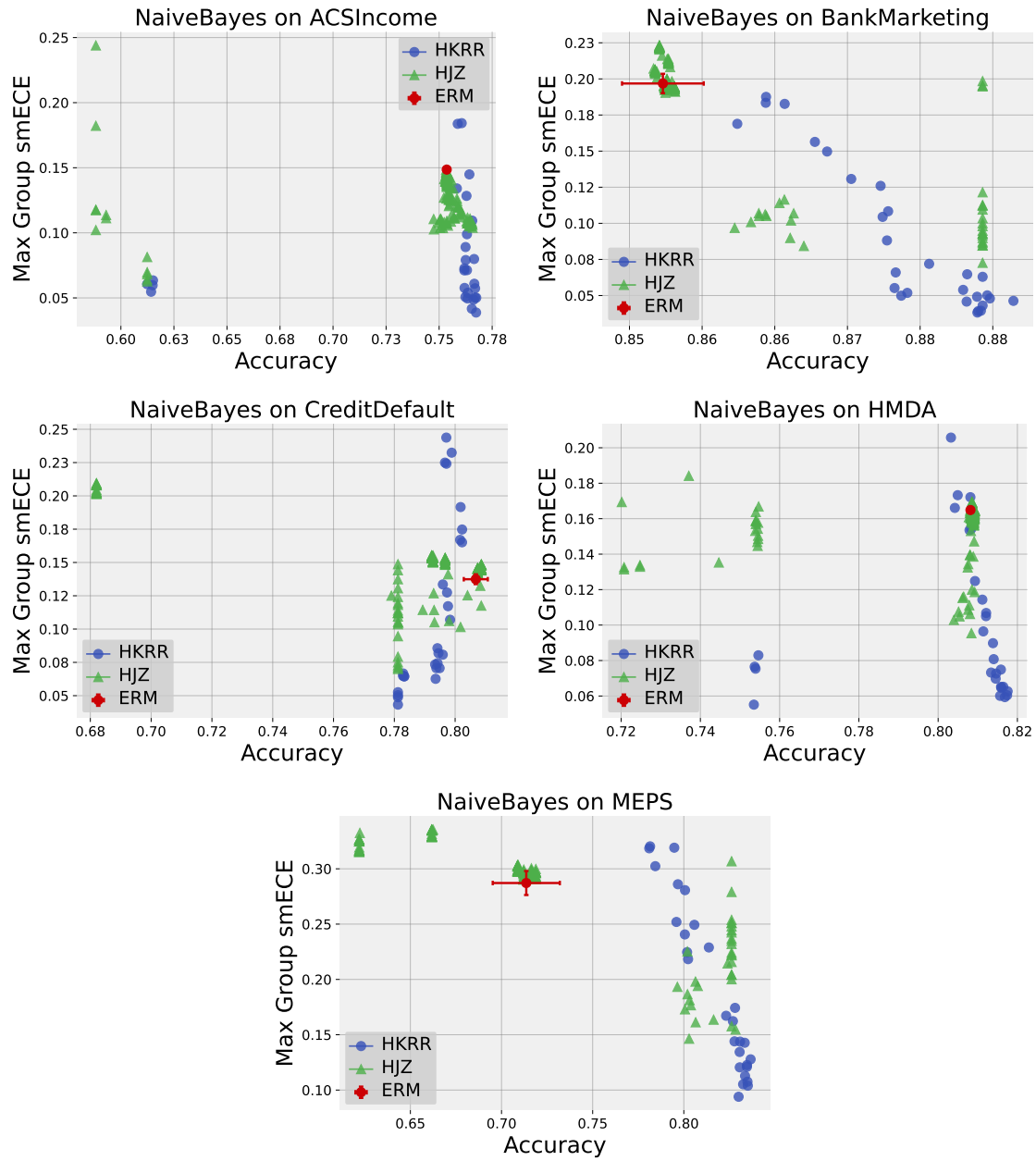


Figure 18: All multicalibration algorithms on Naive Bayes.

F.2 Tables Comparing Best-Performing Multicalibration Algorithms with ERM

Model	ECE ↓	Max ECE ↓	smECE ↓	Max smECE ↓	Acc ↑
MLP ERM	0.01 ± 0.003	0.069 ± 0.011	0.012 ± 0.003	0.058 ± 0.005	0.812 ± 0.001
MLP HKRR	0.023 ± 0.001	0.065 ± 0.004	0.023 ± 0.001	0.063 ± 0.002	0.615 ± 0.0
MLP HJZ	0.01 ± 0.002	0.069 ± 0.008	0.013 ± 0.001	0.055 ± 0.004	0.81 ± 0.002
MLP Platt	0.017 ± 0.009	0.076 ± 0.008	0.018 ± 0.008	0.064 ± 0.008	0.809 ± 0.003
MLP Temp	0.011 ± 0.005	0.068 ± 0.01	0.013 ± 0.004	0.059 ± 0.007	0.811 ± 0.001
MLP Isotonic	0.01 ± 0.001	0.067 ± 0.008	0.011 ± 0.001	0.057 ± 0.002	0.811 ± 0.001
RandomForest ERM	0.01 ± 0.001	0.051 ± 0.01	0.011 ± 0.0	0.046 ± 0.002	0.819 ± 0.001
RandomForest HKRR	0.023 ± 0.001	0.066 ± 0.004	0.023 ± 0.001	0.063 ± 0.002	0.614 ± 0.001
RandomForest HJZ	0.007 ± 0.002	0.052 ± 0.003	0.01 ± 0.001	0.047 ± 0.003	0.818 ± 0.001
RandomForest Platt	0.006 ± 0.001	0.054 ± 0.001	0.01 ± 0.001	0.047 ± 0.002	0.818 ± 0.001
RandomForest Temp	0.027 ± 0.001	0.074 ± 0.008	0.027 ± 0.0	0.061 ± 0.004	0.819 ± 0.001
RandomForest Isotonic	0.008 ± 0.001	0.059 ± 0.011	0.011 ± 0.0	0.048 ± 0.004	0.818 ± 0.001
SVM ERM	0.216 ± 0.001	0.268 ± 0.002	0.109 ± 0.0	0.135 ± 0.001	0.784 ± 0.001
SVM HKRR	0.023 ± 0.001	0.065 ± 0.004	0.023 ± 0.001	0.063 ± 0.002	0.615 ± 0.0
SVM HJZ	0.03 ± 0.002	0.074 ± 0.002	0.026 ± 0.002	0.068 ± 0.006	0.612 ± 0.0
SVM Platt	0.336 ± 0.007	0.403 ± 0.003	0.168 ± 0.004	0.2 ± 0.001	0.664 ± 0.007
SVM Temp	0.022 ± 0.005	0.117 ± 0.005	0.022 ± 0.005	0.117 ± 0.005	0.678 ± 0.006
SVM Isotonic	0.081 ± 0.012	0.155 ± 0.007	0.081 ± 0.012	0.146 ± 0.006	0.664 ± 0.007
LogisticRegression ERM	0.012 ± 0.002	0.065 ± 0.011	0.015 ± 0.002	0.063 ± 0.011	0.779 ± 0.007
LogisticRegression HKRR	0.01 ± 0.001	0.042 ± 0.006	0.01 ± 0.001	0.037 ± 0.002	0.783 ± 0.0
LogisticRegression HJZ	0.011 ± 0.001	0.065 ± 0.005	0.014 ± 0.001	0.057 ± 0.002	0.783 ± 0.001
LogisticRegression Platt	0.023 ± 0.006	0.08 ± 0.019	0.024 ± 0.006	0.076 ± 0.02	0.772 ± 0.011
LogisticRegression Temp	0.02 ± 0.001	0.078 ± 0.005	0.021 ± 0.0	0.072 ± 0.003	0.783 ± 0.0
LogisticRegression Isotonic	0.005 ± 0.001	0.068 ± 0.008	0.009 ± 0.001	0.066 ± 0.009	0.775 ± 0.009
DecisionTree ERM	0.017 ± 0.001	0.066 ± 0.01	0.016 ± 0.001	0.059 ± 0.004	0.804 ± 0.0
DecisionTree HKRR	0.023 ± 0.001	0.065 ± 0.004	0.023 ± 0.001	0.063 ± 0.002	0.615 ± 0.0
DecisionTree HJZ	0.013 ± 0.002	0.064 ± 0.005	0.013 ± 0.001	0.054 ± 0.005	0.803 ± 0.002
DecisionTree Platt	0.015 ± 0.002	0.058 ± 0.004	0.014 ± 0.002	0.055 ± 0.004	0.803 ± 0.002
DecisionTree Temp	0.029 ± 0.002	0.088 ± 0.009	0.028 ± 0.002	0.072 ± 0.006	0.803 ± 0.001
DecisionTree Isotonic	0.007 ± 0.002	0.072 ± 0.01	0.01 ± 0.001	0.057 ± 0.003	0.803 ± 0.001
NaiveBayes ERM	0.117 ± 0.0	0.165 ± 0.0	0.109 ± 0.0	0.149 ± 0.001	0.754 ± 0.0
NaiveBayes HKRR	0.023 ± 0.001	0.065 ± 0.004	0.023 ± 0.001	0.063 ± 0.002	0.615 ± 0.0
NaiveBayes HJZ	0.03 ± 0.002	0.074 ± 0.002	0.026 ± 0.002	0.068 ± 0.006	0.612 ± 0.0
NaiveBayes Platt	0.091 ± 0.004	0.13 ± 0.004	0.086 ± 0.004	0.12 ± 0.003	0.759 ± 0.001
NaiveBayes Temp	0.089 ± 0.003	0.154 ± 0.004	0.087 ± 0.002	0.153 ± 0.004	0.754 ± 0.001
NaiveBayes Isotonic	0.004 ± 0.001	0.094 ± 0.003	0.007 ± 0.0	0.085 ± 0.002	0.769 ± 0.001

Figure 19: ACS Income.

Model	ECE ↓	Max ECE ↓	smECE ↓	Max smECE ↓	Acc ↑
MLP ERM	0.009 ± 0.004	0.048 ± 0.012	0.012 ± 0.002	0.046 ± 0.01	0.901 ± 0.002
MLP HKRR	0.007 ± 0.001	0.044 ± 0.006	0.007 ± 0.002	0.039 ± 0.003	0.879 ± 0.0
MLP HJZ	0.01 ± 0.002	0.043 ± 0.011	0.013 ± 0.002	0.039 ± 0.007	0.9 ± 0.003
MLP Platt	0.01 ± 0.002	0.048 ± 0.012	0.012 ± 0.001	0.044 ± 0.01	0.899 ± 0.001
MLP Temp	0.021 ± 0.006	0.047 ± 0.005	0.022 ± 0.005	0.041 ± 0.003	0.9 ± 0.002
MLP Isotonic	0.014 ± 0.003	0.044 ± 0.009	0.015 ± 0.002	0.04 ± 0.007	0.9 ± 0.0
RandomForest ERM	0.014 ± 0.001	0.045 ± 0.003	0.015 ± 0.0	0.038 ± 0.002	0.903 ± 0.002
RandomForest HKRR	0.007 ± 0.001	0.044 ± 0.006	0.007 ± 0.002	0.039 ± 0.003	0.879 ± 0.0
RandomForest HJZ	0.008 ± 0.001	0.035 ± 0.005	0.011 ± 0.001	0.031 ± 0.003	0.902 ± 0.001
RandomForest Platt	0.01 ± 0.002	0.039 ± 0.002	0.013 ± 0.001	0.033 ± 0.002	0.903 ± 0.001
RandomForest Temp	0.06 ± 0.002	0.084 ± 0.005	0.056 ± 0.001	0.07 ± 0.003	0.899 ± 0.001
RandomForest Isotonic	0.013 ± 0.005	0.037 ± 0.009	0.015 ± 0.004	0.034 ± 0.004	0.902 ± 0.001
SVM ERM	0.106 ± 0.001	0.211 ± 0.019	0.053 ± 0.001	0.106 ± 0.009	0.894 ± 0.001
SVM HKRR	0.007 ± 0.001	0.044 ± 0.006	0.007 ± 0.002	0.039 ± 0.003	0.879 ± 0.0
SVM HJZ	0.003 ± 0.001	0.073 ± 0.005	0.009 ± 0.001	0.073 ± 0.005	0.879 ± 0.0
SVM Platt	0.117 ± 0.001	0.246 ± 0.005	0.059 ± 0.001	0.123 ± 0.003	0.883 ± 0.001
SVM Temp	0.041 ± 0.004	0.091 ± 0.001	0.041 ± 0.004	0.091 ± 0.001	0.879 ± 0.001
SVM Isotonic	0.023 ± 0.009	0.129 ± 0.024	0.023 ± 0.009	0.129 ± 0.023	0.88 ± 0.001
LogisticRegression ERM	0.032 ± 0.001	0.062 ± 0.01	0.03 ± 0.001	0.053 ± 0.002	0.899 ± 0.001
LogisticRegression HKRR	0.007 ± 0.001	0.044 ± 0.006	0.007 ± 0.002	0.039 ± 0.003	0.879 ± 0.0
LogisticRegression HJZ	0.011 ± 0.001	0.045 ± 0.004	0.015 ± 0.001	0.042 ± 0.001	0.9 ± 0.001
LogisticRegression Platt	0.012 ± 0.001	0.049 ± 0.008	0.016 ± 0.001	0.043 ± 0.005	0.899 ± 0.002
LogisticRegression Temp	0.062 ± 0.001	0.088 ± 0.007	0.055 ± 0.001	0.066 ± 0.003	0.899 ± 0.001
LogisticRegression Isotonic	0.009 ± 0.002	0.04 ± 0.006	0.013 ± 0.001	0.036 ± 0.006	0.899 ± 0.002
DecisionTree ERM	0.028 ± 0.002	0.096 ± 0.014	0.022 ± 0.001	0.069 ± 0.003	0.897 ± 0.002
DecisionTree HKRR	0.007 ± 0.001	0.044 ± 0.006	0.007 ± 0.002	0.039 ± 0.003	0.879 ± 0.0
DecisionTree HJZ	0.003 ± 0.001	0.073 ± 0.005	0.009 ± 0.001	0.073 ± 0.005	0.879 ± 0.0
DecisionTree Platt	0.028 ± 0.004	0.086 ± 0.01	0.023 ± 0.003	0.067 ± 0.008	0.897 ± 0.003
DecisionTree Temp	0.056 ± 0.003	0.092 ± 0.01	0.05 ± 0.002	0.073 ± 0.002	0.896 ± 0.002
DecisionTree Isotonic	0.01 ± 0.002	0.06 ± 0.004	0.011 ± 0.002	0.055 ± 0.005	0.896 ± 0.002
NaiveBayes ERM	0.122 ± 0.003	0.271 ± 0.002	0.093 ± 0.002	0.197 ± 0.007	0.857 ± 0.003
NaiveBayes HKRR	0.007 ± 0.001	0.044 ± 0.006	0.007 ± 0.002	0.039 ± 0.003	0.879 ± 0.0
NaiveBayes HJZ	0.003 ± 0.001	0.073 ± 0.005	0.009 ± 0.001	0.073 ± 0.005	0.879 ± 0.0
NaiveBayes Platt	0.121 ± 0.003	0.263 ± 0.006	0.094 ± 0.002	0.195 ± 0.008	0.857 ± 0.002
NaiveBayes Temp	0.083 ± 0.003	0.264 ± 0.008	0.08 ± 0.003	0.24 ± 0.01	0.858 ± 0.002
NaiveBayes Isotonic	0.011 ± 0.003	0.055 ± 0.009	0.014 ± 0.003	0.047 ± 0.006	0.885 ± 0.002

Figure 20: Bank Marketing.

Model	ECE ↓	Max ECE ↓	smECE ↓	Max smECE ↓	Acc ↑
MLP ERM	0.05 ± 0.007	0.104 ± 0.013	0.049 ± 0.006	0.092 ± 0.013	0.824 ± 0.007
MLP HKRR	0.005 ± 0.001	0.08 ± 0.006	0.005 ± 0.001	0.076 ± 0.005	0.754 ± 0.0
MLP HJZ	0.014 ± 0.003	0.076 ± 0.013	0.016 ± 0.002	0.065 ± 0.007	0.829 ± 0.009
MLP Platt	0.132 ± 0.01	0.176 ± 0.013	0.12 ± 0.007	0.149 ± 0.011	0.816 ± 0.008
MLP Temp	0.022 ± 0.007	0.083 ± 0.014	0.022 ± 0.006	0.078 ± 0.013	0.83 ± 0.007
MLP Isotonic	0.009 ± 0.001	0.076 ± 0.011	0.011 ± 0.001	0.071 ± 0.009	0.831 ± 0.007
RandomForest ERM	0.038 ± 0.002	0.099 ± 0.008	0.038 ± 0.002	0.088 ± 0.006	0.868 ± 0.001
RandomForest HKRR	0.013 ± 0.001	0.061 ± 0.019	0.013 ± 0.001	0.047 ± 0.006	0.862 ± 0.002
RandomForest HJZ	0.024 ± 0.003	0.076 ± 0.01	0.024 ± 0.002	0.062 ± 0.008	0.852 ± 0.022
RandomForest Platt	0.017 ± 0.002	0.078 ± 0.009	0.017 ± 0.002	0.069 ± 0.006	0.868 ± 0.001
RandomForest Temp	0.04 ± 0.002	0.061 ± 0.003	0.04 ± 0.001	0.055 ± 0.004	0.867 ± 0.001
RandomForest Isotonic	0.009 ± 0.002	0.058 ± 0.008	0.01 ± 0.002	0.048 ± 0.004	0.869 ± 0.001
SVM ERM	0.144 ± 0.001	0.175 ± 0.004	0.072 ± 0.0	0.088 ± 0.002	0.856 ± 0.001
SVM HKRR	0.005 ± 0.001	0.08 ± 0.006	0.005 ± 0.001	0.076 ± 0.005	0.754 ± 0.0
SVM HJZ	0.051 ± 0.006	0.133 ± 0.006	0.047 ± 0.009	0.133 ± 0.006	0.721 ± 0.02
SVM Platt	0.353 ± 0.003	0.417 ± 0.006	0.175 ± 0.001	0.205 ± 0.002	0.647 ± 0.003
SVM Temp	0.268 ± 0.001	0.288 ± 0.003	0.254 ± 0.001	0.269 ± 0.002	0.631 ± 0.005
SVM Isotonic	0.06 ± 0.049	0.187 ± 0.033	0.044 ± 0.036	0.152 ± 0.028	0.754 ± 0.0
LogisticRegression ERM	0.016 ± 0.001	0.103 ± 0.002	0.016 ± 0.001	0.101 ± 0.002	0.827 ± 0.001
LogisticRegression HKRR	0.012 ± 0.001	0.043 ± 0.01	0.012 ± 0.0	0.04 ± 0.011	0.83 ± 0.002
LogisticRegression HJZ	0.023 ± 0.006	0.084 ± 0.014	0.024 ± 0.006	0.076 ± 0.019	0.833 ± 0.01
LogisticRegression Platt	0.019 ± 0.007	0.079 ± 0.016	0.02 ± 0.006	0.077 ± 0.016	0.831 ± 0.011
LogisticRegression Temp	0.062 ± 0.012	0.1 ± 0.017	0.062 ± 0.01	0.095 ± 0.015	0.832 ± 0.012
LogisticRegression Isotonic	0.004 ± 0.001	0.088 ± 0.018	0.007 ± 0.001	0.087 ± 0.019	0.832 ± 0.012
DecisionTree ERM	0.019 ± 0.001	0.064 ± 0.007	0.018 ± 0.002	0.055 ± 0.006	0.863 ± 0.001
DecisionTree HKRR	0.013 ± 0.002	0.056 ± 0.014	0.013 ± 0.002	0.051 ± 0.011	0.858 ± 0.001
DecisionTree HJZ	0.018 ± 0.002	0.07 ± 0.013	0.017 ± 0.002	0.058 ± 0.007	0.862 ± 0.001
DecisionTree Platt	0.017 ± 0.002	0.073 ± 0.007	0.016 ± 0.001	0.057 ± 0.009	0.863 ± 0.002
DecisionTree Temp	0.064 ± 0.002	0.09 ± 0.007	0.055 ± 0.001	0.07 ± 0.004	0.859 ± 0.001
DecisionTree Isotonic	0.011 ± 0.004	0.066 ± 0.007	0.013 ± 0.003	0.057 ± 0.008	0.86 ± 0.003
NaiveBayes ERM	0.134 ± 0.001	0.199 ± 0.003	0.126 ± 0.0	0.165 ± 0.002	0.808 ± 0.001
NaiveBayes HKRR	0.009 ± 0.002	0.062 ± 0.008	0.009 ± 0.002	0.059 ± 0.009	0.817 ± 0.003
NaiveBayes HJZ	0.052 ± 0.012	0.117 ± 0.013	0.052 ± 0.01	0.108 ± 0.009	0.805 ± 0.003
NaiveBayes Platt	0.124 ± 0.003	0.2 ± 0.009	0.118 ± 0.003	0.168 ± 0.006	0.809 ± 0.002
NaiveBayes Temp	0.174 ± 0.002	0.185 ± 0.001	0.173 ± 0.002	0.177 ± 0.002	0.809 ± 0.0
NaiveBayes Isotonic	0.006 ± 0.001	0.116 ± 0.002	0.009 ± 0.001	0.116 ± 0.002	0.817 ± 0.001

Figure 21: HMDA.

Model	ECE ↓	Max ECE ↓	smECE ↓	Max smECE ↓	Acc ↑
MLP ERM	0.018 ± 0.006	0.116 ± 0.035	0.02 ± 0.005	0.061 ± 0.005	0.819 ± 0.001
MLP HKRR	0.029 ± 0.002	0.057 ± 0.005	0.026 ± 0.001	0.049 ± 0.005	0.781 ± 0.0
MLP HJZ	0.029 ± 0.003	0.086 ± 0.003	0.028 ± 0.002	0.073 ± 0.001	0.781 ± 0.0
MLP Platt	0.028 ± 0.002	0.086 ± 0.001	0.027 ± 0.001	0.075 ± 0.002	0.781 ± 0.0
MLP Temp	0.035 ± 0.008	0.098 ± 0.015	0.035 ± 0.008	0.064 ± 0.004	0.821 ± 0.001
MLP Isotonic	0.003 ± 0.001	0.059 ± 0.001	0.003 ± 0.001	0.059 ± 0.001	0.781 ± 0.0
RandomForest ERM	0.019 ± 0.001	0.112 ± 0.017	0.02 ± 0.001	0.051 ± 0.003	0.82 ± 0.001
RandomForest HKRR	0.029 ± 0.002	0.057 ± 0.005	0.026 ± 0.001	0.049 ± 0.005	0.781 ± 0.0
RandomForest HJZ	0.029 ± 0.003	0.086 ± 0.003	0.028 ± 0.002	0.073 ± 0.001	0.781 ± 0.0
RandomForest Platt	0.027 ± 0.006	0.125 ± 0.028	0.029 ± 0.005	0.07 ± 0.008	0.812 ± 0.01
RandomForest Temp	0.027 ± 0.002	0.071 ± 0.006	0.026 ± 0.001	0.048 ± 0.001	0.82 ± 0.002
RandomForest Isotonic	0.027 ± 0.008	0.114 ± 0.015	0.025 ± 0.006	0.059 ± 0.004	0.818 ± 0.001
SVM ERM	0.181 ± 0.0	0.236 ± 0.002	0.091 ± 0.0	0.118 ± 0.001	0.819 ± 0.0
SVM HKRR	0.029 ± 0.002	0.057 ± 0.005	0.026 ± 0.001	0.049 ± 0.005	0.781 ± 0.0
SVM HJZ	0.029 ± 0.003	0.086 ± 0.003	0.028 ± 0.002	0.073 ± 0.001	0.781 ± 0.0
SVM Platt	0.18 ± 0.0	0.232 ± 0.003	0.09 ± 0.0	0.116 ± 0.001	0.82 ± 0.0
SVM Temp	0.06 ± 0.001	0.088 ± 0.0	0.06 ± 0.001	0.088 ± 0.0	0.819 ± 0.0
SVM Isotonic	0.013 ± 0.005	0.04 ± 0.005	0.013 ± 0.005	0.04 ± 0.004	0.82 ± 0.0
LogisticRegression ERM	0.01 ± 0.001	0.102 ± 0.026	0.015 ± 0.001	0.056 ± 0.002	0.819 ± 0.0
LogisticRegression HKRR	0.029 ± 0.002	0.057 ± 0.005	0.026 ± 0.001	0.049 ± 0.005	0.781 ± 0.0
LogisticRegression HJZ	0.029 ± 0.003	0.086 ± 0.003	0.028 ± 0.002	0.073 ± 0.001	0.781 ± 0.0
LogisticRegression Platt	0.023 ± 0.005	0.114 ± 0.018	0.023 ± 0.004	0.068 ± 0.005	0.817 ± 0.002
LogisticRegression Temp	0.022 ± 0.003	0.101 ± 0.015	0.022 ± 0.002	0.056 ± 0.003	0.819 ± 0.001
LogisticRegression Isotonic	0.009 ± 0.002	0.115 ± 0.026	0.014 ± 0.002	0.06 ± 0.004	0.818 ± 0.001
DecisionTree ERM	0.04 ± 0.003	0.181 ± 0.01	0.031 ± 0.001	0.089 ± 0.006	0.81 ± 0.003
DecisionTree HKRR	0.029 ± 0.002	0.057 ± 0.005	0.026 ± 0.001	0.049 ± 0.005	0.781 ± 0.0
DecisionTree HJZ	0.029 ± 0.003	0.086 ± 0.003	0.028 ± 0.002	0.073 ± 0.001	0.781 ± 0.0
DecisionTree Platt	0.038 ± 0.003	0.138 ± 0.027	0.029 ± 0.003	0.08 ± 0.007	0.811 ± 0.003
DecisionTree Temp	0.077 ± 0.001	0.154 ± 0.015	0.075 ± 0.001	0.103 ± 0.004	0.81 ± 0.003
DecisionTree Isotonic	0.021 ± 0.006	0.084 ± 0.018	0.022 ± 0.005	0.07 ± 0.007	0.811 ± 0.005
NaiveBayes ERM	0.187 ± 0.006	0.248 ± 0.009	0.108 ± 0.005	0.137 ± 0.004	0.807 ± 0.004
NaiveBayes HKRR	0.029 ± 0.002	0.057 ± 0.005	0.026 ± 0.001	0.049 ± 0.005	0.781 ± 0.0
NaiveBayes HJZ	0.029 ± 0.003	0.086 ± 0.003	0.028 ± 0.002	0.073 ± 0.001	0.781 ± 0.0
NaiveBayes Platt	0.197 ± 0.011	0.257 ± 0.012	0.119 ± 0.016	0.154 ± 0.019	0.792 ± 0.014
NaiveBayes Temp	0.07 ± 0.019	0.1 ± 0.023	0.069 ± 0.019	0.097 ± 0.025	0.807 ± 0.003
NaiveBayes Isotonic	0.028 ± 0.006	0.09 ± 0.022	0.027 ± 0.005	0.057 ± 0.008	0.806 ± 0.005

Figure 22: Credit Default.

Model	ECE ↓	Max ECE ↓	smECE ↓	Max smECE ↓	Acc ↑
MLP ERM	0.022 ± 0.006	0.106 ± 0.009	0.024 ± 0.002	0.086 ± 0.015	0.864 ± 0.001
MLP HKRR	0.019 ± 0.005	0.122 ± 0.008	0.019 ± 0.004	0.104 ± 0.002	0.835 ± 0.003
MLP HJZ	0.019 ± 0.003	0.088 ± 0.011	0.021 ± 0.002	0.076 ± 0.018	0.864 ± 0.003
MLP Platt	0.017 ± 0.005	0.1 ± 0.019	0.019 ± 0.003	0.088 ± 0.02	0.865 ± 0.003
MLP Temp	0.019 ± 0.007	0.091 ± 0.016	0.02 ± 0.004	0.081 ± 0.02	0.866 ± 0.001
MLP Isotonic	0.02 ± 0.006	0.108 ± 0.021	0.02 ± 0.004	0.089 ± 0.021	0.864 ± 0.003
RandomForest ERM	0.019 ± 0.001	0.094 ± 0.006	0.021 ± 0.001	0.083 ± 0.004	0.863 ± 0.003
RandomForest HKRR	0.019 ± 0.005	0.122 ± 0.008	0.019 ± 0.004	0.104 ± 0.002	0.835 ± 0.003
RandomForest HJZ	0.021 ± 0.004	0.106 ± 0.011	0.021 ± 0.003	0.101 ± 0.012	0.86 ± 0.003
RandomForest Platt	0.017 ± 0.003	0.093 ± 0.003	0.02 ± 0.001	0.085 ± 0.005	0.861 ± 0.006
RandomForest Temp	0.045 ± 0.003	0.096 ± 0.007	0.045 ± 0.002	0.092 ± 0.009	0.863 ± 0.002
RandomForest Isotonic	0.015 ± 0.002	0.089 ± 0.014	0.017 ± 0.001	0.084 ± 0.014	0.862 ± 0.002
SVM ERM	0.143 ± 0.002	0.376 ± 0.012	0.072 ± 0.001	0.186 ± 0.006	0.857 ± 0.002
SVM HKRR	0.019 ± 0.005	0.122 ± 0.008	0.019 ± 0.004	0.104 ± 0.002	0.835 ± 0.003
SVM HJZ	0.031 ± 0.003	0.156 ± 0.021	0.027 ± 0.004	0.155 ± 0.02	0.828 ± 0.002
SVM Platt	0.14 ± 0.001	0.322 ± 0.019	0.07 ± 0.001	0.161 ± 0.009	0.86 ± 0.001
SVM Temp	0.073 ± 0.008	0.163 ± 0.019	0.073 ± 0.009	0.158 ± 0.015	0.86 ± 0.001
SVM Isotonic	0.048 ± 0.023	0.231 ± 0.085	0.048 ± 0.023	0.218 ± 0.069	0.847 ± 0.017
LogisticRegression ERM	0.022 ± 0.002	0.106 ± 0.008	0.022 ± 0.001	0.083 ± 0.003	0.866 ± 0.002
LogisticRegression HKRR	0.019 ± 0.005	0.122 ± 0.008	0.019 ± 0.004	0.104 ± 0.002	0.835 ± 0.003
LogisticRegression HJZ	0.021 ± 0.003	0.114 ± 0.019	0.023 ± 0.001	0.09 ± 0.011	0.866 ± 0.003
LogisticRegression Platt	0.018 ± 0.003	0.109 ± 0.009	0.021 ± 0.002	0.093 ± 0.017	0.864 ± 0.003
LogisticRegression Temp	0.047 ± 0.002	0.119 ± 0.007	0.044 ± 0.001	0.087 ± 0.003	0.866 ± 0.002
LogisticRegression Isotonic	0.017 ± 0.003	0.109 ± 0.019	0.019 ± 0.003	0.097 ± 0.02	0.863 ± 0.002
DecisionTree ERM	0.067 ± 0.004	0.261 ± 0.028	0.047 ± 0.004	0.166 ± 0.012	0.85 ± 0.006
DecisionTree HKRR	0.019 ± 0.005	0.122 ± 0.008	0.019 ± 0.004	0.104 ± 0.002	0.835 ± 0.003
DecisionTree HJZ	0.031 ± 0.003	0.156 ± 0.021	0.027 ± 0.004	0.155 ± 0.02	0.828 ± 0.002
DecisionTree Platt	0.08 ± 0.005	0.316 ± 0.029	0.054 ± 0.004	0.192 ± 0.009	0.838 ± 0.004
DecisionTree Temp	0.098 ± 0.007	0.214 ± 0.025	0.092 ± 0.005	0.172 ± 0.015	0.838 ± 0.004
DecisionTree Isotonic	0.014 ± 0.003	0.196 ± 0.026	0.015 ± 0.003	0.186 ± 0.027	0.838 ± 0.01
NaiveBayes ERM	0.277 ± 0.019	0.544 ± 0.02	0.164 ± 0.013	0.287 ± 0.011	0.714 ± 0.018
NaiveBayes HKRR	0.019 ± 0.005	0.122 ± 0.008	0.019 ± 0.004	0.104 ± 0.002	0.835 ± 0.003
NaiveBayes HJZ	0.031 ± 0.003	0.156 ± 0.021	0.027 ± 0.004	0.155 ± 0.02	0.828 ± 0.002
NaiveBayes Platt	0.269 ± 0.008	0.535 ± 0.009	0.165 ± 0.004	0.292 ± 0.003	0.719 ± 0.007
NaiveBayes Temp	0.294 ± 0.003	0.368 ± 0.008	0.274 ± 0.002	0.323 ± 0.005	0.719 ± 0.007
NaiveBayes Isotonic	0.019 ± 0.005	0.128 ± 0.017	0.021 ± 0.005	0.122 ± 0.015	0.831 ± 0.006

Figure 23: MEPS.

F.3 Influence of Calibration Fraction on Multicalibration Error and Accuracy

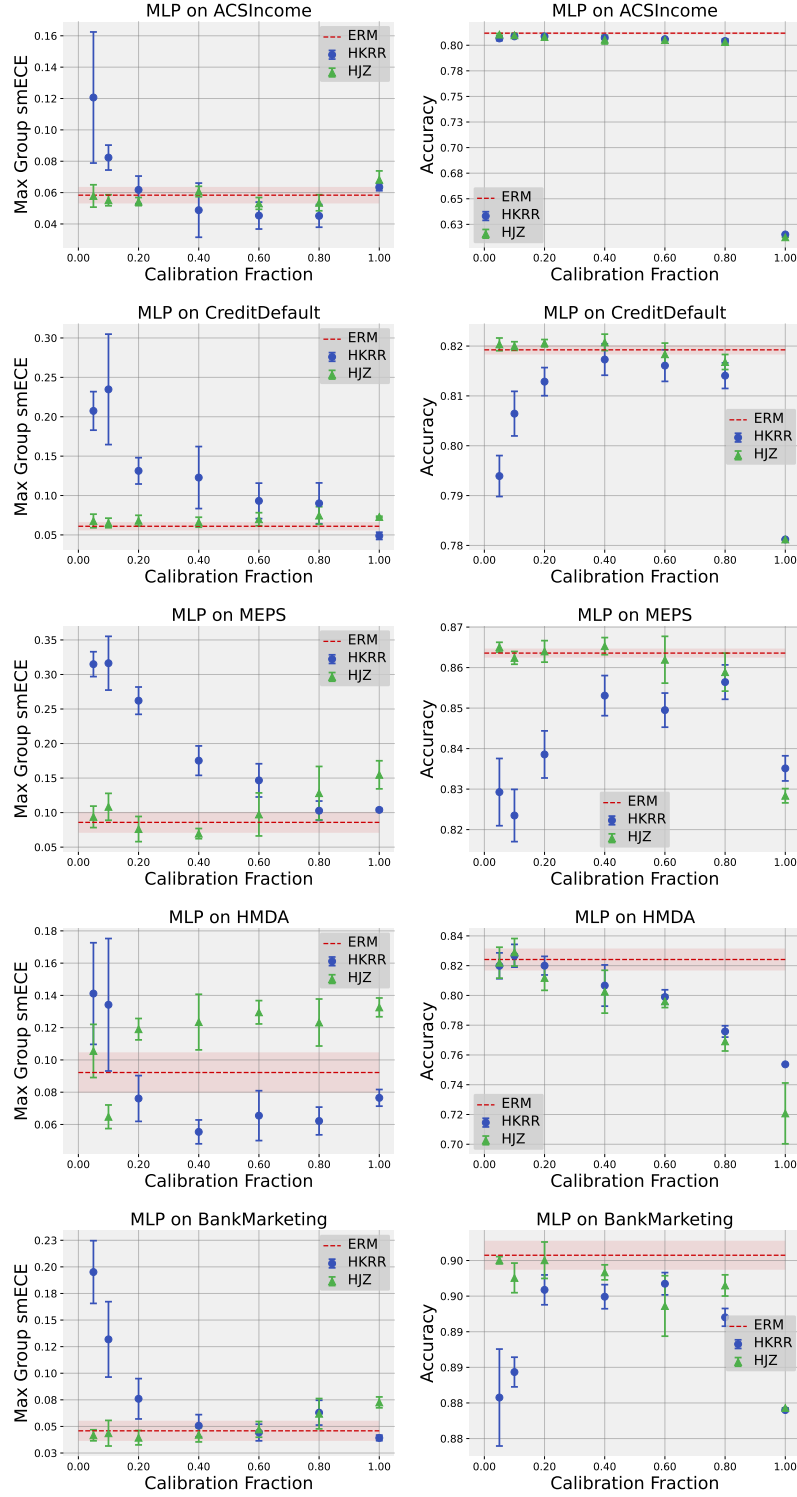


Figure 24: Influence of calibration fraction on MLP multicalibration and accuracy.

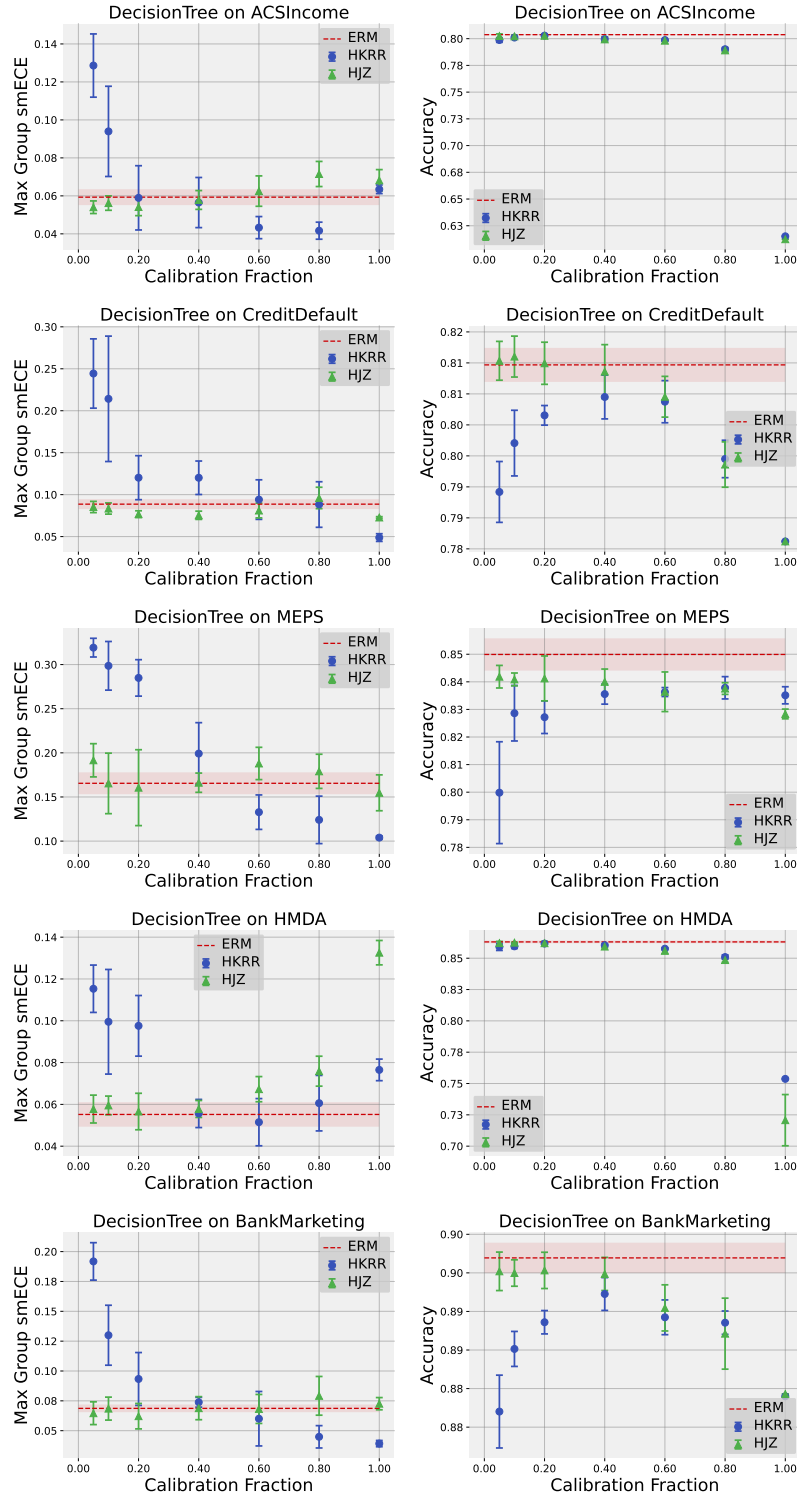


Figure 25: Influence of calibration fraction on decision tree multicalibration.

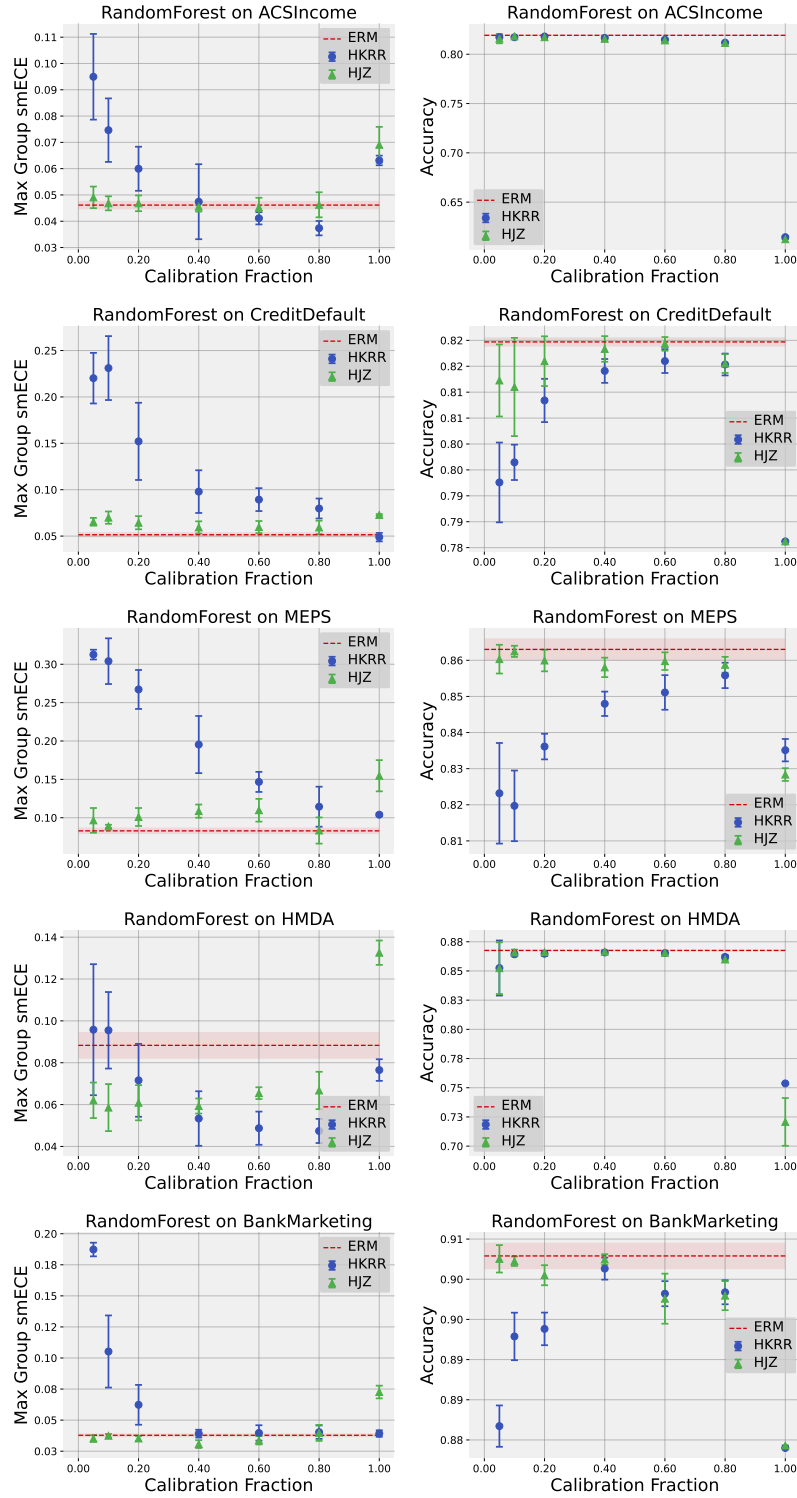


Figure 26: Influence of calibration fraction on RandomForest multicalibration.

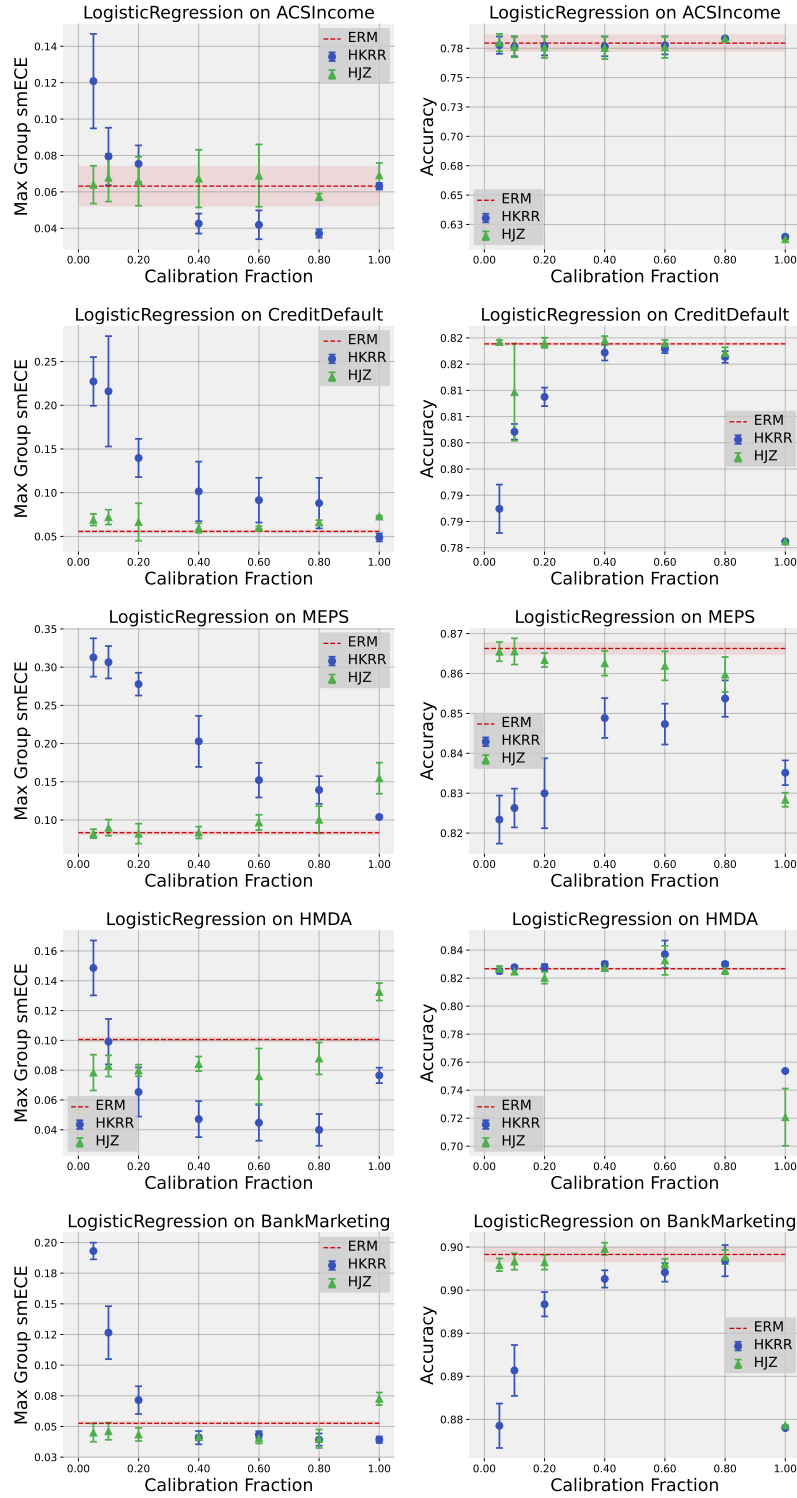


Figure 27: Influence of calibration fraction on LogisticRegression multicalibration.

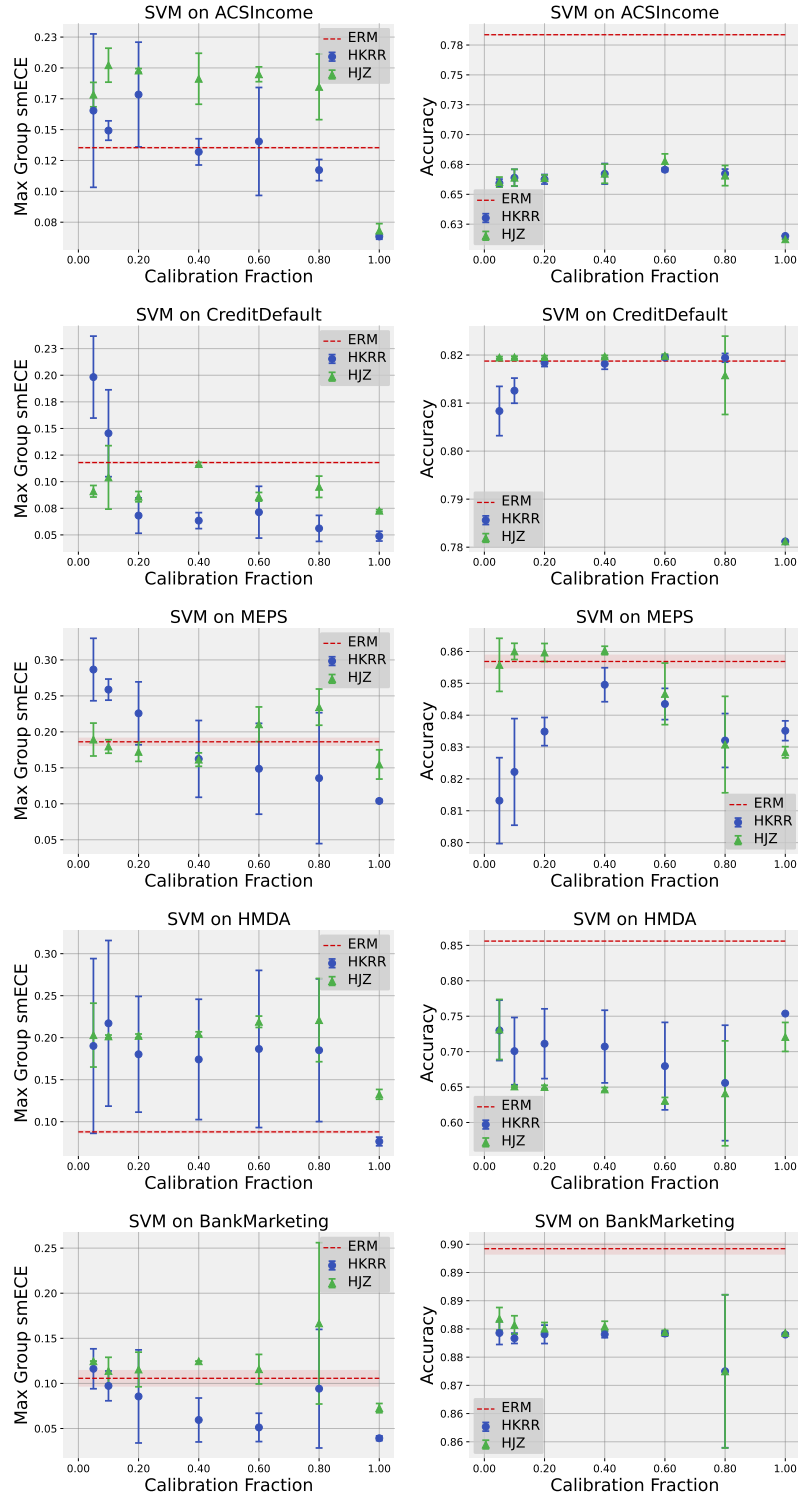


Figure 28: Influence of calibration fraction on SVM multicalibration.

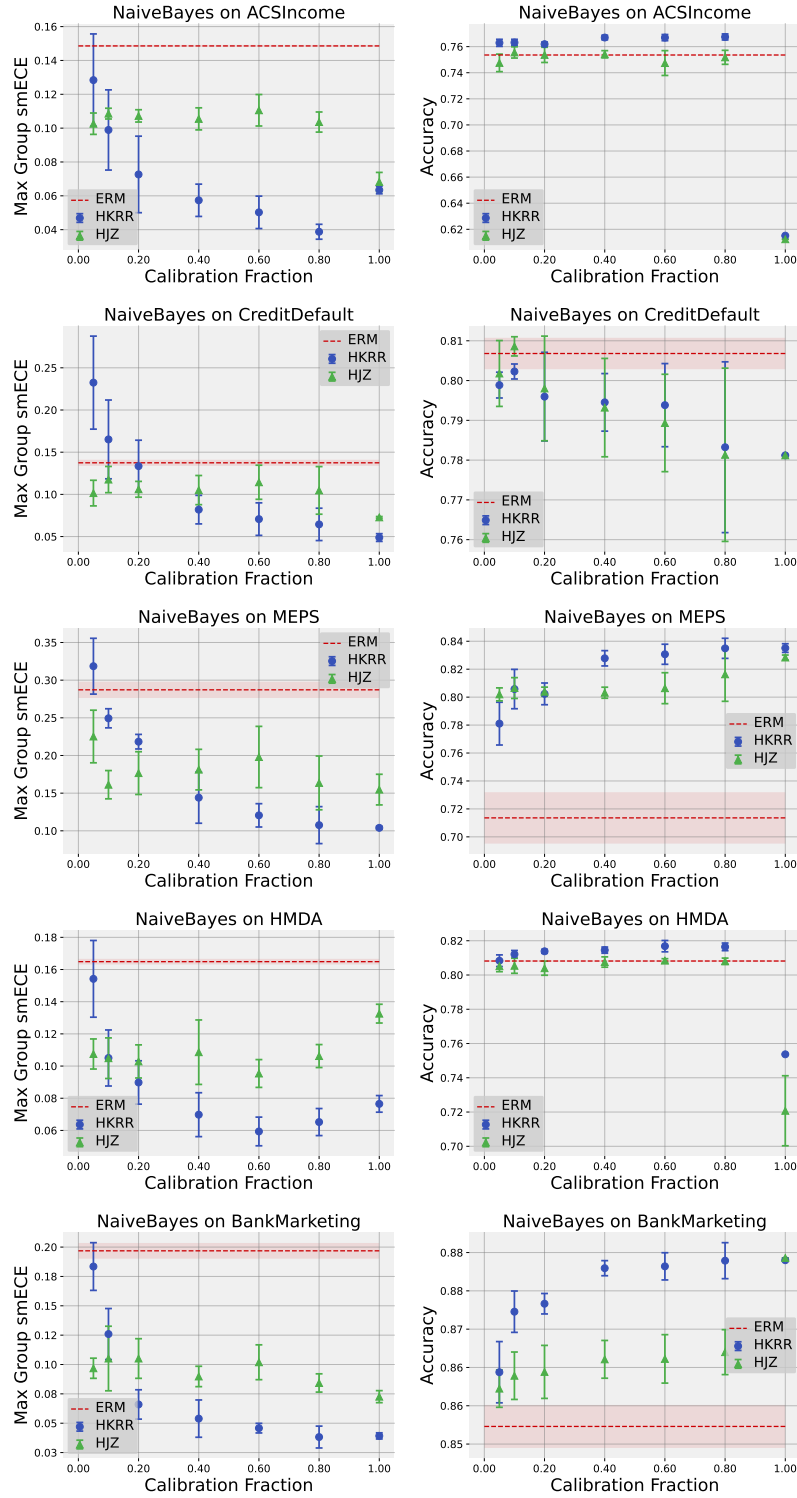


Figure 29: Influence of calibration fraction on NaiveBayes multicalibration.

G Results on Language and Image Datasets

G.1 Plots for All Multicalibration Algorithms

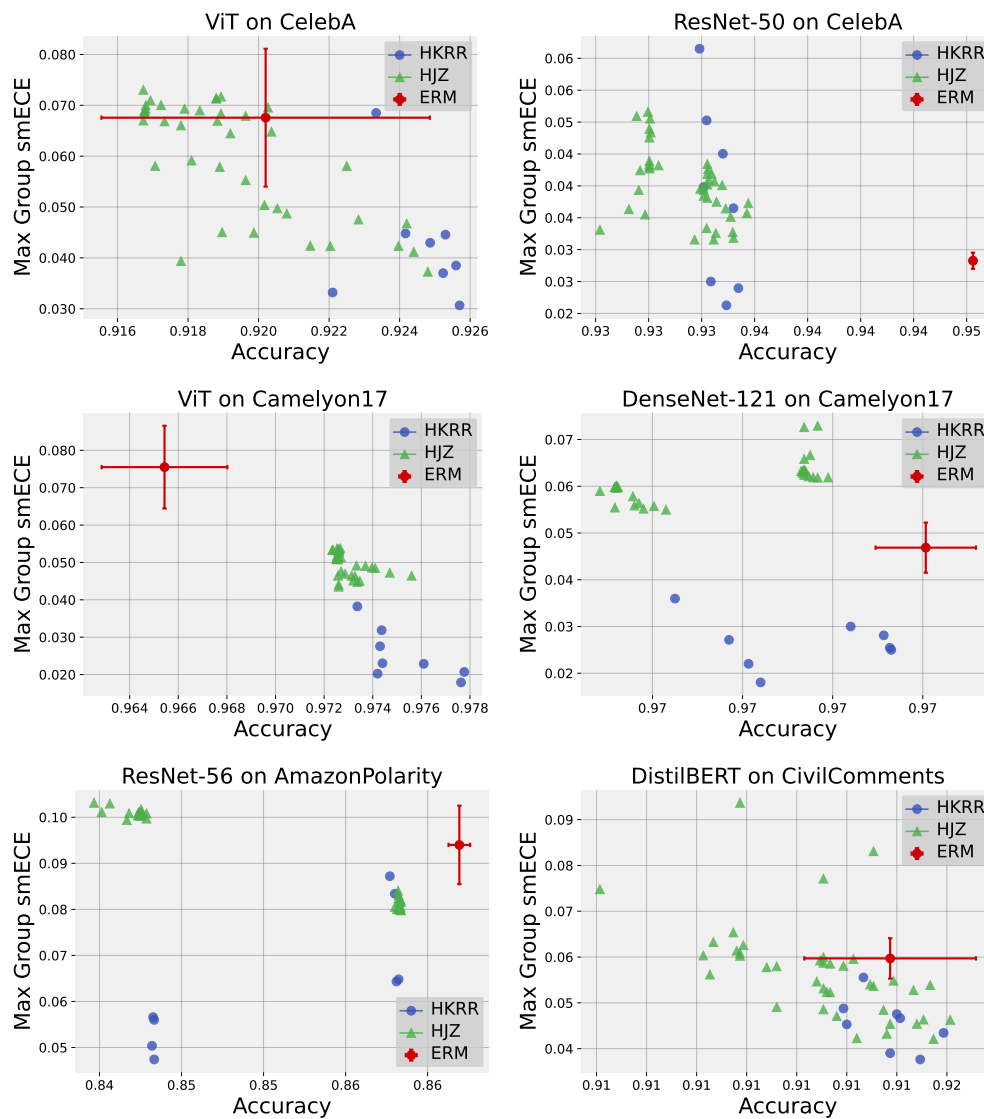


Figure 30: All multicalibration runs for image and language models. Note the small x-axis scale in some plots.

G.2 Result Tables for Image and Language Data

Model	ECE ↓	Max ECE ↓	smECE ↓	Max smECE ↓	Acc ↑
ViT ERM	0.021 ± 0.008	0.076 ± 0.011	0.022 ± 0.007	0.076 ± 0.011	0.965 ± 0.003
ViT HKRR	0.003 ± 0.0	0.018 ± 0.003	0.003 ± 0.0	0.018 ± 0.003	0.978 ± 0.0
ViT HJZ	0.006 ± 0.001	0.047 ± 0.001	0.007 ± 0.001	0.044 ± 0.003	0.973 ± 0.002
ViT Platt	0.014 ± 0.008	0.049 ± 0.014	0.016 ± 0.008	0.049 ± 0.014	0.973 ± 0.003
ViT Temp	0.025 ± 0.004	0.046 ± 0.01	0.019 ± 0.003	0.037 ± 0.008	0.973 ± 0.003
ViT Isotonic	0.001 ± 0.0	0.031 ± 0.007	0.002 ± 0.0	0.031 ± 0.007	0.977 ± 0.001
DenseNet-121 ERM	0.006 ± 0.003	0.047 ± 0.005	0.006 ± 0.002	0.047 ± 0.005	0.974 ± 0.001
DenseNet-121 HKRR	0.003 ± 0.002	0.018 ± 0.002	0.003 ± 0.002	0.018 ± 0.002	0.97 ± 0.003
DenseNet-121 HJZ	0.005 ± 0.001	0.056 ± 0.014	0.006 ± 0.001	0.055 ± 0.014	0.967 ± 0.003
DenseNet-121 Platt	0.006 ± 0.001	0.062 ± 0.015	0.007 ± 0.001	0.062 ± 0.015	0.971 ± 0.002
DenseNet-121 Temp	0.015 ± 0.002	0.052 ± 0.009	0.015 ± 0.002	0.05 ± 0.008	0.967 ± 0.003
DenseNet-121 Isotonic	0.002 ± 0.0	0.047 ± 0.006	0.003 ± 0.0	0.047 ± 0.006	0.972 ± 0.001

Figure 31: Camelyon17.

Model	ECE ↓	Max ECE ↓	smECE ↓	Max smECE ↓	Acc ↑
ViT ERM	0.016 ± 0.006	0.069 ± 0.013	0.016 ± 0.006	0.068 ± 0.014	0.92 ± 0.005
ViT HKRR	0.008 ± 0.003	0.031 ± 0.003	0.008 ± 0.003	0.031 ± 0.003	0.926 ± 0.001
ViT HJZ	0.006 ± 0.001	0.038 ± 0.002	0.009 ± 0.0	0.037 ± 0.002	0.925 ± 0.001
ViT Platt	0.009 ± 0.002	0.047 ± 0.005	0.012 ± 0.002	0.047 ± 0.005	0.924 ± 0.001
ViT Temp	0.028 ± 0.008	0.072 ± 0.012	0.029 ± 0.009	0.07 ± 0.014	0.917 ± 0.006
ViT Isotonic	0.005 ± 0.001	0.057 ± 0.005	0.007 ± 0.001	0.057 ± 0.005	0.922 ± 0.001
ResNet-50 ERM	0.008 ± 0.001	0.028 ± 0.001	0.009 ± 0.001	0.028 ± 0.001	0.945 ± 0.0
ResNet-50 HKRR	0.006 ± 0.001	0.024 ± 0.004	0.006 ± 0.001	0.024 ± 0.004	0.934 ± 0.006
ResNet-50 HJZ	0.006 ± 0.001	0.032 ± 0.003	0.008 ± 0.0	0.033 ± 0.003	0.934 ± 0.007
ResNet-50 Platt	0.005 ± 0.001	0.037 ± 0.004	0.007 ± 0.0	0.037 ± 0.004	0.935 ± 0.006
ResNet-50 Temp	0.017 ± 0.006	0.046 ± 0.006	0.017 ± 0.006	0.045 ± 0.006	0.933 ± 0.007
ResNet-50 Isotonic	0.003 ± 0.001	0.051 ± 0.009	0.006 ± 0.001	0.051 ± 0.009	0.933 ± 0.007

Figure 32: CelebA.

Model	ECE ↓	Max ECE ↓	smECE ↓	Max smECE ↓	Acc ↑
DistilBERT ERM	0.021 ± 0.001	0.065 ± 0.005	0.021 ± 0.001	0.06 ± 0.004	0.915 ± 0.001
DistilBERT HKRR	0.013 ± 0.0	0.047 ± 0.005	0.013 ± 0.0	0.043 ± 0.004	0.915 ± 0.001
DistilBERT HJZ	0.004 ± 0.001	0.043 ± 0.008	0.007 ± 0.001	0.043 ± 0.007	0.915 ± 0.001
DistilBERT Platt	0.004 ± 0.001	0.047 ± 0.008	0.007 ± 0.0	0.045 ± 0.007	0.915 ± 0.001
DistilBERT Temp	0.025 ± 0.005	0.044 ± 0.004	0.025 ± 0.005	0.044 ± 0.004	0.914 ± 0.001
DistilBERT Isotonic	0.002 ± 0.0	0.032 ± 0.006	0.005 ± 0.0	0.032 ± 0.006	0.916 ± 0.0

Figure 33: Civil Comments.

Model	ECE ↓	Max ECE ↓	smECE ↓	Max smECE ↓	Acc ↑
ResNet-56 ERM	0.039 ± 0.013	0.094 ± 0.009	0.039 ± 0.013	0.094 ± 0.009	0.867 ± 0.001
ResNet-56 HKRR	0.015 ± 0.001	0.059 ± 0.01	0.015 ± 0.001	0.047 ± 0.005	0.848 ± 0.004
ResNet-56 HJZ	0.013 ± 0.005	0.081 ± 0.012	0.014 ± 0.005	0.081 ± 0.012	0.863 ± 0.002
ResNet-56 Platt	0.009 ± 0.003	0.082 ± 0.01	0.01 ± 0.002	0.082 ± 0.01	0.863 ± 0.002
ResNet-56 Temp	0.024 ± 0.01	0.07 ± 0.003	0.024 ± 0.01	0.069 ± 0.003	0.863 ± 0.002
ResNet-56 Isotonic	0.005 ± 0.001	0.079 ± 0.009	0.007 ± 0.0	0.078 ± 0.008	0.863 ± 0.002

Figure 34: Amazon Polarity.